DETERMINATION OF NATURAL RADIOACTIVITY IN THE SOIL OF OMARURU, NAMIBIA

A MINI THESIS

SUBMITTED IN PARTIAL FULFILMENT

OF THE REQUIREMENTS FOR THE DEGREE OF

MASTER OF SCIENCE IN NUCLEAR SCIENCE

OF

THE UNIVERSITY OF NAMIBIA

BY

MERCEY MBUENDE

200926241

APRIL 2022

Supervisor: Professor J. A. Oyedele (Department of Physics, University of Namibia)

Co-Supervisor: Mr S. A. Shimboyo (Department of Physics, University of Namibia)

ABSTRACT

In this study, the level of natural radioactivity and associated hazards has been evaluated for 50 soil samples from the town of Omaruru in western Namibia. Activity concentrations ($Bqkg^{-1}$) of the primordial radionuclides ^{238}U, ^{232}Th and ^{40}K in these soil samples were determined using a gamma-ray spectroscopy system with a High Purity Germanium detector (HPGe). These activity concentrations of the primordial radionuclides were calculated by using the intensities of selected gamma lines in the spectra as emitted by the radionuclides. The samples were collected from ten geographical areas which are inhabited localities in the town. The obtained results of activity concentrations for every soil sample was compared with the worldwide average values as recommended by UNSCEAR 2000. The values of activity concentration of ^{238}U have been found to lie in the range of 39.4 - 111.1 Bq kg^{-1}, with an average value of 63.9 ± 15.4 Bq kg^{-1}, the values of activity concentration of ^{232}Th ranged from 49.5 - 231.7 Bq kg^{-1} with an average value of 120.0 ± 42.9 Bq $kg^{-1}$and the values of activity concentration of ^{40}K ranged from 692.4 - 1425.5 Bq kg^{-1}, with an average value of 1136.7 ± 197.8 Bq kg^{-1}. The absorbed dose rates and annual effective dose as well as the radiation hazard indices in the soil samples, were calculated by employing the determined activity concentration values of ^{238}U, ^{232}Th and ^{40}K. The total absorbed dose rate varied from 90.9 to 230.2 $nGyh^{-1}$, with the average value of 149.4 ± 35.2 $nGyh^{-1}$ and subsequently the annual effective dose ranged between 0.112 to 0.282 $mSvy^{-1}$, with an average value of 0.183 ± 0.043 $mSvy^{-1}$. This result of the annual effective dose is much lower than the recommended maximum permissible dose rate of 1.0 $mSvy^{-1}$. The implication thereof is that the town of Omaruru has a normal background radiation. Additionally, the average value of the radium equivalent activity was 323.0 ± 80.2 Bq kg^{-1}, and is lower than the recommended maximum value of 370 Bq kg^{-1}. Furthermore, the average external hazard index, which was 0.87 ± 0.22, is also below the

recommended safe level of 1. Based on these results, the radiological hazard is low in Omaruru. The results obtained in this study would be useful in establishing a baseline data to serve as a future reference in confirming possible changes in the environmental radioactivity as a result of any nuclear and related activities.

DEDICATION

This thesis is dedicated to my late father and mother, Likius Seuakouje Muukua and Priscilla Kapimbua Mbuende Muukua. I am because you were.

To my dear husband, Marvelous Marvin Tjazuko, there is a road, no simple highway, between the dawn and the dark of night. I'm glad you're here to walk it with me.

ACKNOWLEDGEMENTS

Firstly, I would like to thank The Creator for the blessing of life.

To my husband, family and friends, thank you for the support and inspiration to become an achiever.

My supervisor, Professor James Akindele Oyedele thank you for training, guidance and invaluable supervision and comments for successfully completion of this project work.

My co-supervisor, Mr. Simon Andrew Shimboyo, thank you for all you have done to make this a reality.

I would also like to express my heartfelt thanks to everyone that was instrumental in the production of this Thesis, my colleagues from the National Radiation Protection Authority (NRPA).

I thank my fellow comrades Mbeurora Sebastiaan Tjitombo, Deidre Visser, Shaleen Mbuende, Soetman Mbuende and McLee Karupa for their immense moral support and energy as volunteer assistants who selflessly stood by me during sample preparation.

The author would also like to thank the following institutions for their contributions;

University of Namibia: Department of Physics and Faculty of Science at the University of Namibia, Windhoek.

International Atomic Energy Agency

Ministry of Health and Social Services: National Radiation Protection Authority

Municipality of Omaruru

Erongo Regional Council

DECLARATIONS

I, Mercey Mbuende, hereby declare that this study is my own work and is a true reflection of my research, and that this work, or any part thereof has not been submitted for a degree at any other institution.

…… …….. …….

Name and Surname Signature Date and Place

List of Important Abbreviations and Definitions

ADC - Analog Digital Converter

Absorbed dose - Fundamental dosimetric quantity defined as the energy imparted by ionizing radiation in unit mass of matter; measured in grays (Gy); 1 gray is equal to 1 joule per kilogram (J/kg).

Activity - The rate at which spontaneous transformations occur in a given amount of radioactive material. (Strictly, the expectation value of the number of nuclear transformations occurring in a given quantity of material per unit time). It is measured in becquerels (Bq); 1 becquerel equals one transformation per second.

Bequerel (Bq) - The SI unit of activity, equal to one transformation per second. As the unit is so small, multiples are frequently used such as megabecquerels (MBq) which is 10^6 or a million becquerels. (1 GBq is 10^9 Bq; 1 TBq is 10^{12} Bq; and 1 PBq is 10^{15} Bq)

BDL - Below Detection Limit

Dose - A measure of the energy deposited by radiation in a target. Dose can be used as a shorthand for absorbed dose and effective dose when the context is clear.

FWHM - Full Wave at Half Maximum

HPGe - High Purity Germanium

IAEA	-	International Atomic Energy Agency
ICRP	-	International Commission on Radiological Protection
ICRU	-	International Commission on Radiological Units and Measurements
KeV	-	Kilo Electron-Volt
LLD	-	Lowest Limit of Detection
MCA	-	Multi-Channel Analyzer
MDA	-	Minimal Detectable Activity
MPD	-	Maximum Permissible Dose
NORM	-	Naturally Occurring Radioactive Material
NRPA	-	National Radiation Protection Authority
SRM	-	Standard Reference Material
UNSCEAR	-	United Nations Scientific Committee on the Effects of Atomic Radiation
WHO	-	World Health Organization
µm	-	micrometer

List of Tables

List of Figures

Table of Contents

1. Chapter 1: Introduction

1.1. Background of the study

Radioactivity is a phenomenon in which an unstable nucleus spontaneous disintegrates spontaneously to form a different nucleus and, in the process, emits ionizing radiation. Radionuclides on the earth are categorize as either primordial or naturally occurring, cosmogenic or anthropogenic. Primordial radionuclides such as ^{232}Th, ^{238}U and ^{40}K, in the soil, generate a significant component of the background radiation or natural radioactivity to which the population is exposed [1]. Exposure to ionizing radiation can have adverse effects on the population especially when the concentrations of radionuclides in the soil are high. For this reason, many scientists worldwide have studied the background radiation in different towns and countries [1-7]. In the case of Namibia, there is a wealth of mineral resources, including uranium, which may lead to a high and hazardous background radiation level in some areas or towns. Consequently, a research group in the Department of Physics of the University of Namibia has studied the natural radioactivity in many towns in the uranium-rich Erongo region or western Namibia with the support of the National Radiation Protection Authority (NRPA) and the International Atomic Energy Agency (IAEA) [2]. However, the Group has not studied the natural radioactivity in the important town of Omaruru in western Namibia. This study therefore investigates the natural radioactivity level in the town of Omaruru, Namibia.

1.2. Statement of the problem

Several studies have been done on the activity concentrations of natural radionuclides in the soils of various towns in Namibia [2, 4] and the results obtained are being used to provide a database of activity concentrations in the soils of Namibia. However, there is limited data available on the

activity concentrations of radionuclides or on natural radioactivity in the soil of Omaruru while the radioactivity in most of the other towns in the uranium-rich Erongo region has been studied. Hence, there is a need to study natural radioactivity and the associated hazard in the soil of Omaruru and use the results obtained to improve the database of activity concentrations.

1.3. Objectives of the study

The objectives of this study are to

a) determine the activity concentrations and activity ratios of the primordial radionuclides ^{40}K, ^{232}Th and ^{238}U in the soil of Omaruru.
b) determine the radium equivalent activity and the mean annual effective dose for the town of Omaruru and ascertain whether or not the town has normal background radiation.
c) contribute to baseline data of radionuclide concentrations in the soils of Erongo region.

1.4. Significance of the study

Omaruru is a town in the Erongo region of Namibia, which is a region well known for its vast uranium (^{238}U) resources. The town is located between 15º and 16° east longitude, and 21º and 21º 30' south latitude. The town is inhabited and frequently visited by Indigenous, Western descendants (Afrikaners), European and other international people. It is well known for its annual festival where the Ovaherero people commemorate the deaths of their past local chiefs and for the dinosaur footprints at a nearby farm, called Otjihenamaparero.

The inhabitants will know the level of background radiation to which they are exposed and if it is high, the municipality and subsequently the relevant authority (i.e NRPA) would be informed. Omaruru has vast areas which are characterized by material of the Damara granite intrusions,

Damara Supergroup and Gariep complex [8]. High radiation levels are associated with granites, therefore it is desirable to determine the level of the background radiation to which visitors and the inhabitants of the town are exposed and to compare the level to those of other towns in a uranium-rich region [9].

This study will provide information on the radioactivity level in the town and also contribute to the baseline data of activity concentrations in the soils of western Namibia.

2. Chapter 2: Literature Review

2.1.Introduction

This chapter reflects the current state of knowledge on which this study is based. Different literature will be reviewed as taken from various books, scientific journals and published articles. Firstly, there will be a discussion on the atomic nuclei and radioactivity. In addition, environmental radioactivity will also be discussed. Followed by detailed review of interaction of radiation with matter and the biological effects of radiation. This chapter will also study the quantification of radionuclides and the tools used. In conclusion, various literature on both local and international studies on natural radioactivity in soil will also be presented.

2.2.Radioactive decay and Radioactivity

Radioactivity occurs when certain nuclides undergo spontaneous disintegration and energy (in the form of radiation) is liberated in the process. New nuclides are formed in the process and radiations such as gamma rays, alpha particles and beta particles are emitted.

Of the nuclei found on Earth, the vast majority is stable. This is so because almost all short-lived radioactive nuclei have decayed during the history of the Earth. There are approximately 270 stable isotopes and 50 naturally occurring radioisotopes (radioactive isotopes). Thousands of other radioisotopes have been made in the laboratory.

Protons are positively charged and repel one another electrically. Therefore, an excess of neutrons which produce only an attractive force, is required for stability, thus leading to $N > Z$ for stable nuclei. There is a limit to the ability of neutrons to prevent the disruption of the nucleus by the Coulomb repulsion. This phenomenon therefore leads to instability of nuclei.

The instability can also be attributed to the unstable configurations due to the filling of quantum states by the nucleon [10]. Because of their instability, some nuclei undergo decay processes, termed radioactive decay, to transition to a more stable constellation of its nuclear constituent. The Chart of the Nuclides, part of which is shown in Figure 2.1, is a plot of nuclei as a function of proton number, Z, and neutron number, N. All stable nuclei and known radioactive nuclei, both naturally occurring and manmade, are shown on this chart, along with their decay properties. Nuclei with an excess of protons or neutrons in comparison with the stable nuclei will decay toward the stable nuclei by changing protons into neutrons or neutrons into protons, or else by shedding neutrons or protons either singly or in combination. Nuclei are also unstable if they are excited, that is, not in their lowest energy states. In this case the nucleus can decay by getting rid of its excess energy without changing Z or N by emitting a gamma ray.

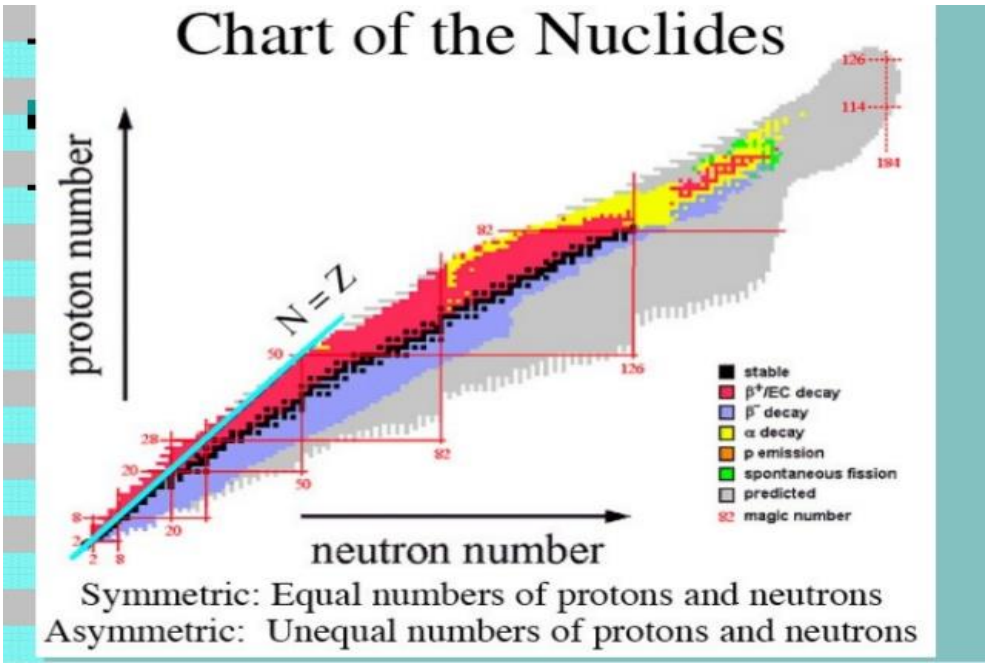

Figure 2.1.: Chart of Nuclides [10]

Nuclear decay processes must satisfy several conservation laws, meaning that the value of the conserved quantity after the decay, taking into account all the decay products, must equal the same quantity evaluated for the nucleus before the decay. Conserved quantities include total energy (including mass), electric charge, linear and angular momentum, number of nucleons, and lepton number (sum of the number of electrons, neutrinos, positrons and antineutrinos—with antiparticles counting as -1).

The probability that a particular nucleus will undergo radioactive decay during a fixed length of time does not depend on the age of the nucleus or how it was created. Although the exact lifetime of one particular nucleus cannot be predicted, the mean (or average) lifetime of a sample containing many nuclei of the same isotope can be predicted and measured. A convenient way of determining the lifetime of an isotope is to measure how long it takes for one-half of the nuclei in a sample to decay—this quantity is called the half-life, $t_{1/2}$. Of the original nuclei that did not decay, half will decay if we wait another half-life, leaving one-quarter of the original sample after a total time of two half-lives. After three half-lives, one-eighth of the original sample will remain and so on. Measured half-lives vary from tiny fractions of seconds to billions of years, depending on the isotope.

The number of nuclei in a sample that will decay in a given interval of time is proportional to the number of nuclei in the sample. This condition leads to radioactive decay showing itself as an exponential process, as shown in Figure 2.2. The number, N of the original nuclei remaining after a time t from an original sample of N_0 nuclei is

$$N = N_0 e^{-(t_{1/2}/T)}$$

where T is the mean lifetime of the parent nuclei. From this relation, it can be shown that

$t_{1/2}$= 0.693T

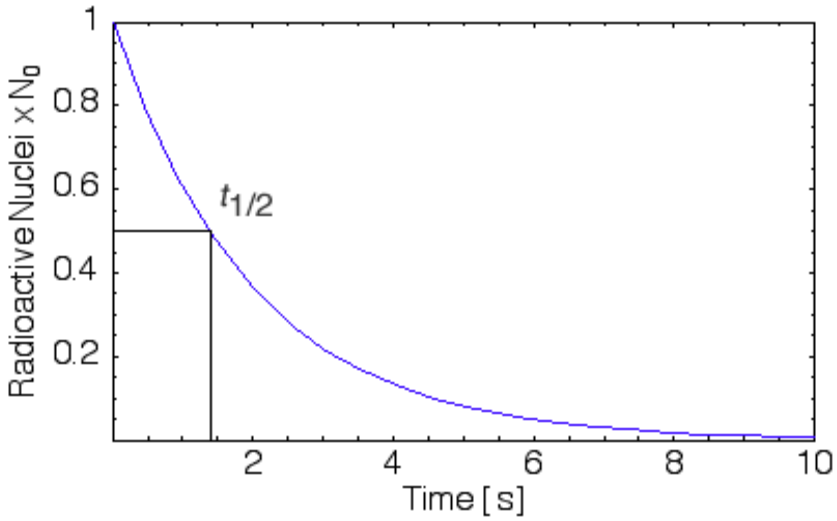

Figure 2.2: Radioactive decay curve [11]

Radioactive decay will change one nucleus to another if the product nucleus has a greater nuclear binding energy than the initial decaying nucleus. The difference in binding energy (comparing the initial decaying nucleus and the product nucleus) determines which decays are energetically possible and which are not. The excess binding energy appears as kinetic energy or rest mass energy of the decay products.

The main categories are: (i) alpha (α) decay, (ii) beta (β) decay encompassing three related decay processes (beta minus, beta plus and electron capture) and (iii) gamma (γ) decay encompassing two competing decay processes (pure γ decay and internal conversion). The three less important radioactive decay categories are: (i) spontaneous fission, (ii) proton emission decay and (iii) neutron emission decay. Nuclides with an excess number of neutrons are referred to as neutron-rich, while nuclides with an excess number of protons are referred to as proton-rich. The following features are notable:

- for a slight proton–neutron imbalance in the nucleus, radionuclides decay by β decay characterized by transformation of a proton into a neutron in β+ decay, and transformation of a neutron into a proton in β– decay.
- for a large proton–neutron imbalance in the nucleus, the radionuclides decay by emission of nucleons: α particles in α decay, protons in proton emission decay and neutrons in neutron emission decay.
- or very large atomic mass number nuclides (A > 230), spontaneous fission, which competes with α decay, is also possible [12].

Excited nuclei decay to their ground state through γ decay. Most of these transformations occur immediately upon production of the excited state by either α or β decay. However, a few exhibit delayed decays that are governed by their own decay constants and are referred to as metastable states (e.g. ^{99m}Tc). Nuclear transformations are usually accompanied by emission of energetic particles (charged particles, neutral particles, photons, etc.). The particles released in the various decay modes are as follows:

- Alpha particles in α decay;
- Electrons in β– decay;
- Positrons in β+ decay;
- Neutrinos in β+ decay;
- Antineutrinos in β– decay;
- Gamma rays in γ decay;
- atomic orbital electrons in internal conversion;
- Neutrons in spontaneous fission and in neutron emission decay;

— heavier nuclei in spontaneous fission;

— Protons in proton emission decay.

In each nuclear transformation, a number of physical quantities must be conserved. The most important of these quantities are: (i) total energy, (ii) momentum, (iii) charge, (iv) atomic number and (v) atomic mass number (number of nucleons). The total energy of particles released by the transformation process is equal to the net decrease in the rest energy of the neutral atom, from parent P to daughter d. The disintegration (decay) energy, often referred to as the Q value for the radioactive decay, is defined as follows:

$$Q = \{M(P) - [M(D) + m]\}\ c^2$$

where M(P), M(D) and *m* are the nuclear rest masses (in unified atomic mass units u) of the parent, daughter and emitted particles, respectively.

For radioactive decay to be energetically possible, the Q value must be greater than zero. This means that spontaneous radioactive decay processes release energy and are called exoergic or exothermic. For Q > 0, the energy equivalent of the Q value is shared as kinetic energy between the particles emitted in the decay process and the daughter product. Since the daughter generally has a much larger mass than the other emitted particles, the kinetic energy acquired by the daughter is usually negligibly small [12].

2.2.1. Alpha decay

In α decay, a radioactive parent nucleus P decays into a more stable daughter nucleus D by ejecting an energetic α particle. Since the α particle is a ^{4}He nucleus ($^4_2He^{2+}$), in α decay the parent's atomic number Z decreases by two and its atomic mass number A decreases by four:

$$^A_ZP \rightarrow {}^{A-4}_{Z-2}D + {}^4_2He^{2+} = {}^{A-4}_{Z-2}D + \alpha$$

In alpha decay, the atomic number changes, so the original (or parent) atoms and the decay-product (or daughter) atoms are different elements and therefore have different chemical properties. In the alpha decay of a nucleus, the change in binding energy appears as the kinetic energy of the alpha particle and the daughter nucleus. Because this energy must be shared between these two particles, and because the alpha particle and daughter nucleus must have equal and opposite momenta, the emitted alpha particle and recoiling nucleus will each have a well-defined energy after the decay. Because of its smaller mass, most of the kinetic energy goes to the alpha particle. Naturally occurring α particles have kinetic energies between 4 and 9 MeV; their range in air is between 1 and 10 cm, and their range in tissue is between 10 and 100 μm.

Typical examples of α decay are the decay of ^{226}Ra with a half-life of 1602 a into ^{222}Rn (as shown in Figure 2.3 below) which is also radioactive and decays with a half-life of 3.82 d into ^{218}Po.

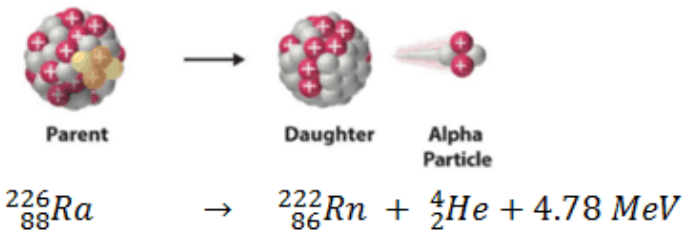

Figure 2.3: Alpha decay of ^{226}Ra [13]

2.2.2. Beta minus decay

Beta particles are electrons or positrons (electrons with positive electric charge, or antielectrons). Beta decay occurs when, in a nucleus with too many protons or too many neutrons, one of the protons or neutrons is transformed into the other.

In beta minus (β^-) decay, a neutron-rich parent nucleus P transforms a neutron into a proton and ejects an electron e– and an electronic antineutrino, as shown in Figure 2.4. Thus, in β^- decay, the atomic number of the daughter increases by one while the atomic mass number remains constant.

A typical example of β^- decay is the decay of ^{60}Co with a half-life of 5.26 a into an excited state of ^{60}Ni plus an electron and an electron antineutrino. The decay is initially to a nuclear excited state of ^{60}Ni, from which it emits either one or two γ rays in γ decay to reach the ground state of the ^{60}Ni isotope.

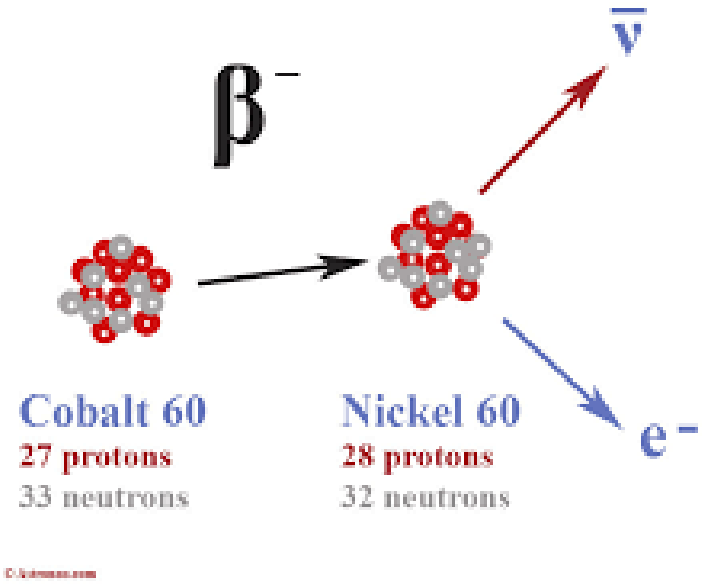

Figure 2.4: β^- decay is the decay of ^{60}Co [13]

2.2.3. Beta plus decay

In beta plus decay, shown in Figure 2.5, a proton decays into a neutron, a positron, and a neutrino: $p \rightarrow n + e^{+} + \nu$

The radioactive nuclide which is rich in protons, converts a proton to a neutron and a positron.

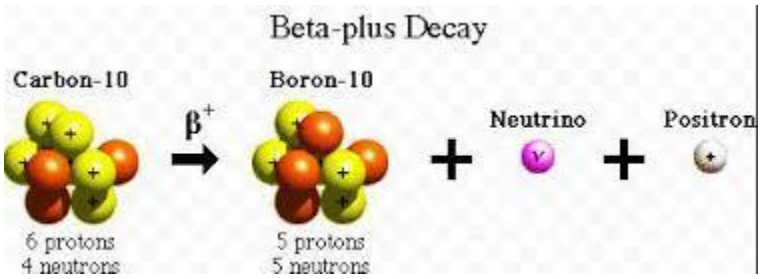

Figure 2.5: Beta plus decay [14]

Proton decay, neutron decay, and electron capture are three ways in which protons can be changed into neutrons or vice-versa; in each decay there is a change in the atomic number, so that the parent and daughter atoms are different elements. In all three processes, the number A of nucleons remains the same, while both proton number, Z, and neutron number, N, increase or decrease by 1.

2.2.4. Gamma Decay

Gamma (γ) decay encompasses two competing decay processes which is pure gamma decay and internal conversion.

In pure gamma decay, an unstable radionuclide dissipates energy by emitting gamma rays. However, there is no change in the number of protons and neutrons in the nuclide as shown in Figure 2.6.

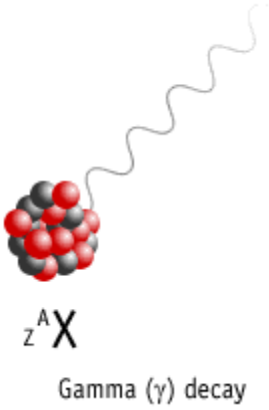

Figure 2.6: Pure gamma decay [14]

Internal conversion is a radioactive decay process wherein an excited nucleus interacts electromagnetically with one of the orbital electrons of the atom. This causes the electron to be ejected from the atom [14]. Thus, in an internal conversion process, a high-energy electron is emitted from the radioactive atom, but not from the nucleus. Since an electron is lost from the atom, a hole appears in an electron shell which is subsequently filled by other electrons that descend to that empty, lower energy level, and in the process emit characteristic X-ray(s), Auger electron(s), or both. The atom thus emits high-energy electrons and X-ray photons, none of which originate in the nucleus as illustrated in Figure 2.7.

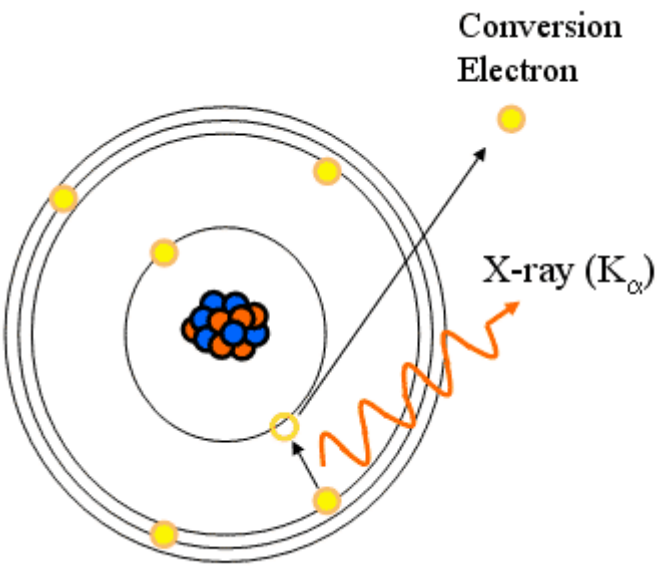

Figure 2.7: Electron conversion in gamma decay [12]

2.3. Environmental Radioactivity

Radioactivity on the earth can be categorized according to three different types, namely those of cosmogenic, primordial and anthropogenic nature [15].

- Cosmogenic radionuclides – primary radiation (protons and other heavier nuclei), originating from outer space, called cosmic rays continuously bombard stable atoms in the atmosphere and create radionuclides (e.g. ^{22}Na, ^{7}Be and ^{14}C). Essentially all nuclear species lighter than the target nuclei (primarily nitrogen, oxygen and argon) are produced by high-energy spallation interactions. When cosmic rays strike the atmosphere, they produce a nuclear cascade or a shower of secondary particles. Production is greatest in the upper stratosphere, but some energetic cosmic-ray neutrons and protons survive in the lower atmosphere, producing cosmogenic radionuclides there as well. Production is not only altitude- but also latitude-dependent and varies as well with the 11-year solar cycle that modulates cosmic-ray penetration

through the earth's magnetic field. Most of these are eventually stopped before they reach the surface of the earth except for energetic muons (μ), and neutrons (n), which may penetrate all the way into the earth. Except for ^{3}H, ^{14}C, and ^{22}Na, which are elements with metabolic roles in the human body, the cosmogenic radionuclides contribute little to radiation doses and are mainly of relevance as tracers in the atmosphere and in hydrological systems after deposition.

- Anthropogenic radionuclides – these are man-made radionuclides released into the environment through, for example, the testing of nuclear weapons, nuclear reactor accidents (e.g. Chernobyl) and in the radio-isotope manufacturing industry (^{137}Cs, ^{90}Sr and ^{131}I).
- Naturally occurring radionuclides of terrestrial origin (also called primordial radionuclides) are present in various degrees in all media in the environment, including the human body itself. Primordial radionuclides have half-lives sufficiently long that they have existed since the formation of the earth, and from the radioactive decay of these, secondary radionuclides are produced (e.g. ^{40}K, ^{232}Th, and ^{238}U). Irradiation of the human body from external sources is mainly by gamma radiation from radionuclides in the ^{238}U and ^{232}Th series and from ^{40}K. These radionuclides are also present in the body and irradiate the various organs with alpha and beta particles, as well as gamma rays. Some other terrestrial radionuclides, including those of the ^{235}U series, ^{87}Rb, ^{138}La, ^{147}Sm, and ^{176}Lu, exist in nature but at such low levels that their contributions to the dose in humans are small. Physical data for terrestrial radionuclides are included in Table 2.1.

Element	Isotope	Half-Life	Decay Mode
		Cosmogenic Radionuclides	
Hydrogen	^{3}H	12.33 a	beta (100%)
Beryllium	^{7}Be	53.29 d	EC (100%)
	^{10}Be	$1.51\ 10^{6}$ a	beta (100%)
Carbon	^{14}C	5730 a	beta (100%)
Sodium	^{22}Na	2.602 a	EC(100 %)
Aluminium	^{26}Al	$7.4\ 10^{5}$ a	EC(100 %)
Silicon	^{32}Si	172 a	beta (100%)
Phosphorus	^{32}P	14.26 d	beta (100%)
	^{33}P	25.34 d	beta (100%)
Sulphur	^{35}S	87.51 d	beta (100%)
Chlorine	^{36}Cl	$3.01\ 10^{5}$ a	EC (1.9 %). Beta (98.1%)
Argon	^{37}Ar	35.04 d	EC(100 %)
	^{39}Ar	269 a	beta (100%)
Krypton	^{81}Kr	$2.29\ 10^{5}$ a	EC(100 %)
		Terrestrial Radionuclides	
Potassium	^{40}K	$1.28\ 10^{9}$ a	beta (89.3%), EC (10.7%)
Rubidium	^{87}Rb	$4.75\ 10^{10}$ a	beta (100%)
Lanthanum	^{138}La	$1.05\ 10^{11}$ a	beta (33.6%), EC (66.4%)
Samarium	^{147}Sm	$1.06\ 10^{11}$ a	alpha (100%)
Lutecium	^{176}Lu	$3.73\ 10^{10}$ a	beta (100%)
^{238}U series: Uranium	^{238}U	$4.47\ 10^{9}$ a	alpha (100%)
Thorium	^{234}Th	24.10 d	beta (100%)
Protactinium	^{234m}Pa	1.17 m	beta (99.8%), IT [b]
Uranium	^{234}U	$2.45\ 10^{5}$ a	alpha (100%)
Thorium	^{230}Th	$7.54\ 10^{4}$ a	alpha (100%)
Radium	^{226}Ra	1600 a	alpha (100%)
Radon	^{222}Rn	3.824 d	alpha (100%)
Polonium	^{218}Po	3.05 m	alpha (99.98%), beta (0.02%)
Lead	^{214}Pb	26.8 m	beta (100%)
Bismuth	^{214}Bi	19.9 m	alpha (0.02), beta (99.98%)
Polonium	^{214}Po	164 µs	alpha (100%)
Lead	^{210}Pb	22.3 a	beta (100%)
Bismuth	^{210}Bi	5.013 d	beta (100%)
Polonium	^{210}Po	138.4 d	alpha (100%)
Lead	^{206}Pb	Stable	

^{232}Th series: Thorium	^{232}Th	1.405 10^{10} a	alpha (100%)
Radium	^{228}Ra	5.75 a	beta (100%)
Actinium	^{228}Ac	6.15 h	beta (100%)
Thorium	^{228}Th	1.912 a	alpha (100%)
Radium	^{224}Ra	3.66 d	alpha (100%)
Radon	^{220}Rn	55.6 s	alpha (100%)
Polonium	^{216}Po	0.145 s	alpha (100%)
Lead	^{212}Pb	10.64 h	beta (100%)
Bismuth	^{212}Bi	60.55 m	alpha (36%), beta (64%)
Polonium	^{212}Po	0.299 μs	alpha (100%)
Thalium	^{208}Tl	3.053 m	beta (100%)
Lead	^{208}Pb	Stable	
^{235}U series: Uranium	^{235}U	7.038 10^{8} a	alpha (100%)
Thorium	^{231}Th	25.52 h	beta (100%)
Protactinium	^{231}Pa	32760 a	alpha (100%)
Actinium	^{227}Ac	21.77 a	alpha(1.4%), beta (98.6%)
Thorium	^{227}Th	18.72 d	alpha (100%)
Francium	^{223}Fr	21.8 m	beta (100%)
Radium	^{223}Ra	11.44 d	alpha (100%)
Radon	^{219}Rn	3.96 s	alpha (100%)
Polonium	^{215}Po	1.781 ms	alpha (100%)
Lead	^{211}Pb	36.1 m	beta (100%)
Bismuth	^{211}Bi	2.14 m	alpha (99.7%), beta (0.3%)
Thalium	^{207}Tl	4.77 m	beta (100%)
Lead	^{207}Pb	Stable	

a Electron capture.

b Internal transition.

Table 2.1 Physical data for radionuclides of natural origin [16]

Uranium was isolated by Martin Heinrich Klaproth in 1789 from the mineral pitchblende. At that time uranium was not considered as particularly dangerous and was used for colouring pottery and glass. In 1896 Henri Becquerel observed that uranium was emitting invisible rays that fogged a photographic plate as if it was exposed to daylight. In honour of his discovery of radioactivity, the unit for radioactivity is given the name Becquerel (Bq), corresponding to one disintegration per second. Natural uranium mainly contains ^{238}U (99.27%), which is the parent of a decay series schematically presented in Table 2.1. As shown in this Table 2.1 each member of this series is unstable and decays by either alpha or beta emission until stable ^{206}Pb has been formed. Besides ^{238}U, natural uranium contains 0.73% ^{235}U. This isotope is also the parent of a decay series ending at ^{207}Pb.

Thorium was extracted by Jöns Jakob Berzelius in 1829 from a mineral that nowadays is known as thorite ($ThSiO_4$). Thorium oxide has found wide application in e.g. gas mantles which, when heated, emit a bright white light. In 1898 the radioactivity of thorium was demonstrated by Gerhard Schmidt and confirmed later that year by Marie Curie. Like ^{235}U and ^{238}U, ^{232}Th heads a decay chain, but ends at another stable isotope of lead (^{208}Pb). The principal decay scheme is shown in Table 2.1 along with the type of decay. In most materials the parent nuclides ^{235}U, ^{238}U and ^{232}Th are nearly in a state of secular equilibrium with their decay products, meaning that the activities of all radionuclides within a series are equal. In case a building material (or a major constituent) is a residue of chemical processing, for instance gypsum from phosphate production units, certain radionuclides can be specifically enriched or depleted. The secular equilibrium is then violated and the initially single decay series will be split up in several smaller sub-series headed by longer-lived radionuclides. As indicated in

Table 2.1 some members of the series decay by beta emission. After emission of a beta particle, the nucleus may still be slightly unstable and the excess energy is released by one or more gamma rays. Besides radionuclides from the decay series of ^{238}U and ^{232}Th, also ^{40}K contributes to the indoor exposure due to gamma radiation. It is an isotope of the element potassium.

Potassium was discovered by Humphry Davy in 1807 and named so after the material from which he isolated it: potash. Natural potassium comprises three isotopes, ^{39}K, ^{40}K and ^{41}K of which only ^{40}K is radioactive. Its abundance in nature is limited to 0.012% and it decays to stable ^{40}Ar (11.2%) and ^{40}Ca (88.8%) [17]

The worldwide average annual exposure to natural radiation sources is 2.4 mSv [18]

2.4. Interaction of radiation with matter

Radiation is called ionizing if it has sufficient energy to remove one or several electrons from an atom. In this process an atom that was previously intact and charge neutral is turned into an ion. An ion is defined as an atom that is missing one or several electrons, which implies that it is no longer charge-neutral. Ionising radiation interacts with matter by:

- Interaction with the electron cloud of the atom, or by
- Interaction with the nucleus of the atom.

Ionising radiation can be electrically charged particles such as alpha-particles and beta-particles as well as electrons, or it can be uncharged particles and radiation quanta such as neutrons and ionising photons. The mode of interaction, range in matter and penetrating ability of charged and uncharged particles differ considerably.

A mono-energetic, parallel beam of charged particles has a well-defined range in a given material, therefore these are often directly ionizing. These charged particles interact continuously and intensely, display a well-defined range, and are not nearly as deeply penetrating as uncharged particles. When charged particles such as alpha-particles and free electrons interact with atoms, they lose energy in two ways — ionisation slowing down and radiative slowing down.

Uncharged particles (including gamma rays, x-rays and neutrons) are attenuated more or less exponentially, without having a well-defined range, and in so doing, these are not directly ionizing and ionization occurs through secondary effects.

2.4.1. Ionisation slowing down of charged particles

Coulombic interactions of charged particles with atomic electrons, can impart energy to the atom and excite it to a higher energy state. If the energy transfer of the charged particle to the atomic electrons is sufficiently high, one or more electrons may be detached from the atom. This is called ionisation. In every ionisation event, a small amount of energy is transferred from the charged particle to the atom being ionised, so that the energy of the moving particle decreases, i.e. it is slowed down [12]. This process is called ionisation slowing down.

2.4.2. Radiative slowing down

The second mechanism by which charged particles are slowed down will now be discussed. If a charged particle which is free, (i.e. not bound in a potential well) enters the vicinity of an atomic nucleus, it will be deflected from its original direction, by the electric field of the

nucleus. This causes a rapid change in the direction as well as the speed of movement of the electrically charged projectile. When an unbound, free, electrically charged particle is decelerated, it emits ionising photons known as bremsstrahlung ("braking radiation") [12]. In contrast, charged particles such as atomic electrons that are bound inside a potential well, have quantised energies and do not emit bremsstrahlung when they are accelerated. This process by which charged particles lose energy and slow down, is called radiative slowing down. The faster the deceleration, the more bremsstrahlung is produced.

2.4.3. Alpha Radiation

Alpha radiation is normally produced from the radioactive decay of heavy nuclides and from certain nuclear reactions. The alpha particle consists of 2 neutrons and 2 protons, so it is essentially the same as the nucleus of a helium atom. Because it has no electrons, the alpha particle has a charge of +2. This positive charge causes the alpha particle to strip electrons from the orbits of atoms in its vicinity. As the alpha particle passes through material, it removes electrons from the orbits of atoms it passes near. Energy is required to remove electrons and the energy of the alpha particle is reduced by each reaction. Eventually the particle will expend its kinetic energy, gain 2 electrons in orbit, and become a helium atom. Because of its strong positive charge and large mass, the alpha particle deposits a large amount of energy in a short distance of travel. This rapid, large deposition of energy limits the penetration of alpha particles. The most energetic alpha particles are stopped by a few centimeters of air or a sheet of paper.

2.4.4. Beta-minus Radiation

A beta-minus particle is an electron that has been ejected at a high velocity from an unstable nucleus. An electron has a small mass and an electrical charge of -1. Beta particles cause ionization by displacing electrons from orbits. The ionization occurs from collisions with orbiting electrons. Each collision removes kinetic energy from the beta particle, causing it to slow down. Eventually the beta particle will be slowed enough to allow it to be captured as an orbiting electron in an atom. Although more penetrating than the alpha, the beta is relatively easy to stop and has a low power of penetration. Even the most energetic beta radiation can be stopped by a few millimeters of metal.

2.4.5. Positron Radiation

Positively charged electrons are called positrons. Except for the positive charge, they are identical to beta-minus particles and interact with matter in a similar manner. Positrons are very short-lived, however, and are quickly annihilated by interaction with a negatively charged electron, producing two gammas with a combined energy (calculated below) equal to the rest mass of the positive and negative electrons.

$$2\ electrons\left(\frac{0.000549\ amu}{electron}\right)\left(\frac{931.5\ Mev}{amu}\right) = 1.02\ MeV$$

2.4.6. Neutron radiation

Neutrons have no electrical charge. They have nearly the same mass as a proton (a hydrogen atom nucleus). A neutron has hundreds of times more mass than an electron, but 1/4 the mass of an alpha particle. The source of neutrons is primarily nuclear reactions, such as fission, but

they may also be produced from the decay of radioactive nuclides. Because of its lack of charge, the neutron is difficult to stop and has a high penetrating power.

Neutrons are attenuated (reduced in energy and numbers) by three major interactions, elastic scatter, inelastic scatter, and absorption. In elastic scatter, a neutron collides with a nucleus and bounces off. This reaction transmits some of the kinetic energy of the neutron to the nucleus of the atom, resulting in the neutron being slowed, and the atom receives some kinetic energy (motion). This process is sometimes referred to as "the billiard ball effect."

As the mass of the nucleus approaches the mass of the neutron, this reaction becomes more effective in slowing the neutron. Hydrogenous material attenuates neutrons most effectively.

In the inelastic scatter reaction, the same neutron/nucleus collision occurs as in elastic scatter. However, in this reaction, the nucleus receives some internal energy as well as kinetic energy. This slows the neutron, but leaves the nucleus in an excited state. When the nucleus decays to its original energy level, it normally emits a gamma ray.

In the absorption reaction, the neutron is actually absorbed into the nucleus of an atom. The neutron is captured, but the atom is left in an excited state. If the nucleus emits one or more gamma rays to reach a stable level, the process is called radiative capture. This reaction occurs at most neutron energy levels, but is more probable at lower energy levels.

2.4.7. Gamma Radiation

Gamma radiation is electromagnetic radiation. It is commonly referred to as a gamma ray and is very similar to an x-ray. The difference is that gamma rays are emitted from the nucleus of an atom, and x-rays are produced by orbiting electrons. The x-ray is produced when orbiting

electrons move to a lower energy orbit or when fast-moving electrons approaching an atom are deflected and decelerated as they react with the atom's electrical field (called Bremsstrahlung). The gamma ray is produced by the decay of excited nuclei and by nuclear reactions. Because the gamma ray has no mass and no charge, it is difficult to stop and has a very high penetrating power.

There are three methods of attenuating gamma rays. The first method is referred to as the **photo-electric effect**. When a low energy gamma strikes an atom, the total energy of the gamma is expended in ejecting an electron from orbit. The result is ionization of the atom and expulsion of a high energy electron. The emitted electron or photoelectron will have a kinetic energy which is equal to the difference in the energy of the photon and the binding energy of the electron (which is energy binding the electron to the atom). That is,

$$K.E = h\upsilon - B.E$$

where K.E is the kinetic energy of the emitted electron, $h\upsilon$ is the energy of the photon and B.E is binding energy of the ejected electron. The ejected electron is usually from the K- or L- shell of the atom. The use of materials with high atomic numbers Z (such as lead) as gamma-ray shielding and in detectors is due to this severe dependence of the photoelectric absorption probability on the atomic number of the absorber material [18].

This reaction is most predominant with low energy gammas interacting in materials with high atomic weight and rarely occurs with gammas having an energy above 1 MeV. Any gamma energy in excess of the binding energy of the electron is carried off by the electron in the form of kinetic energy.

The second method of attenuation of gammas is called **Compton scattering**. The gamma interacts with an orbital or free electron; however, in this case, the photon loses only a fraction of its energy. The actual energy loss depending on the scattering angle of the gamma. The gamma continues on at lower energy, and the energy difference is absorbed by the electron. This reaction becomes important for gamma energies of about 0.1 MeV and higher.

At higher energy levels, a third method of attenuation is predominant. This method is **pair-production**. When a high energy gamma passes close enough to a heavy nucleus, the gamma completely disappears, and an electron and a positron are formed. For this reaction to take place, the original gamma must have at least 1.02 MeV energy. Any energy greater than 1.02 MeV becomes kinetic energy shared between the electron and positron. The probability of pair-production increases significantly for higher energy gammas [11].

2.5. Biological effects of radiation

The interaction of ionizing radiation with biological material results in ionizations and excitations of molecules and atoms, which may cause molecular changes in the DNA in the cell nucleus. The induced damage includes single- and double-strand breaks in the DNA sugar-phosphate backbone and a variety of modifications in DNA bases. Although the cells possess very efficient mechanisms for signalling and repairing the induced DNA damage, there is a small chance for unrepaired or misrepaired double-strand breaks, thought to be a principal lesion that may lead to modification of healthy cells into malignant ones. Both frequency and complexity of the damage depend on the linear energy transfer (LET) of the radiation, the radiation energy lost per unit of path in the material. As indicated in the previous paragraph inhabitants are exposed to alpha and gamma radiation, examples of high-LET and low-LET

radiation, respectively. High-LET radiation will produce more complex, closely spaced damage, which will be less repairable and more likely to result in chromosomal abnormalities and gene mutations. Besides various DNA repair pathways, the cellular response to DNA damage also includes arrest at one of several cell-cycle checkpoints and onset of apoptosis, i.e. the active biochemical process of programmed cell death. These two processes prevent the propagation of damaged cells and thus offer an additional protection of an individual against tumour formation. Recent summaries of the biological and epidemiological information on radiation-related cancer risk are given by ICRP and the National Research Council's Committee on the Biological Effects of Ionizing Radiation [19].

2.5.1. Linear Non- Threshold Theory

The induction of a radiation-induced cancer is taken to be probabilistic in nature, with no threshold, and in a way that is proportional to the radiation dose. This is known as the linear, non-threshold theory (LNT). Given the uncertainties at low doses, it seems to be unlikely that epidemiological studies will establish the presence or absence of a threshold. Most of the epidemiological data originates from studies of large populations exposed to high doses of ionizing radiation, such as the survivors of the nuclear disaster in Fukushima. A common feature of these studies is that they show that the risk associated with the exposure to ionizing radiation is directly proportional to the dose as illustrated in Figure 2.8 below.

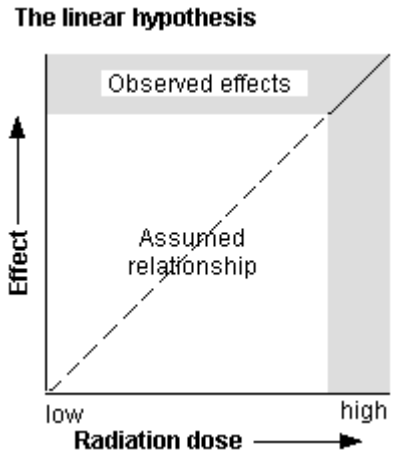

Figure 2.8: Linear relationship between risk and dose for high exposures [12]

This is confirmed for exposure doses greater than 0.1 Sv = 100mSv. However, for exposures less than 100 mSv, the data is insufficient to prove that the linear relationship between the exposure dose and the associated risk also applies to low-level exposures [20].

2.5.2. Radiobiological effects

Biological effects as a result of exposure to ionizing radiation depend on the exposure dose, and the period over which the exposure occurred. Radiobiological effects, which is the actual biological effects resulting from the exposure to ionizing radiation, are divided into the so called *stochastic effects*, and *deterministic effects*. Radiobiological effects on people are termed *somatic effects*, those on embryos and foetuses are termed *teratogenic effects*, and hereditary effects on offspring are called *genetic effects*. These will be discussed as follows:

- **Deterministic Effects**

  These are effects arising from the exposure to ionizing radiation which occurs only above a fixed threshold dose, which is usually an acute dose, as shown in Figure 2.9.

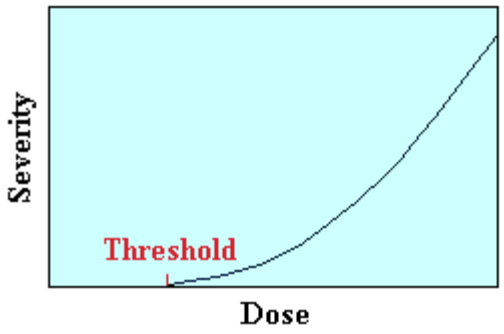

Figure 2.9.: Relationship between severity of effects and radiation dose [12].

Above the threshold dose, the severity of deterministic effects (injury or the impairment of the capacity for tissue recovery) increases with dose [16]. Below the threshold, the deterministic effects do not occur. Examples of deterministic effects include:

- Radiation burns (Figure 2.10)
- Cataract induction (Figure 2.11)
- Acute radiation syndrome

Figure 2.10: Radiation skin burns [13]

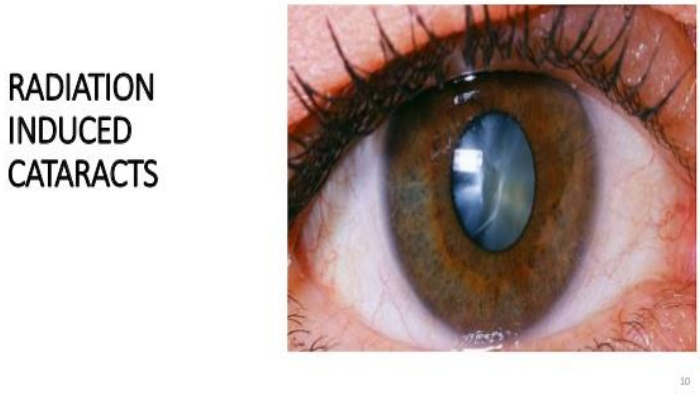

Figure 2.11: Radiation induced cataract [13]

- **Stochastic Effects**

  These are effects resulting from the random exposure to ionizing radiation and have no threshold dose. In addition, there is no certainty as to when they will occur, and who is most likely to be affected. The severity of the effect is independent of the dose, but the probability of the effect is proportional to the dose received, as shown in Figure 2.12.

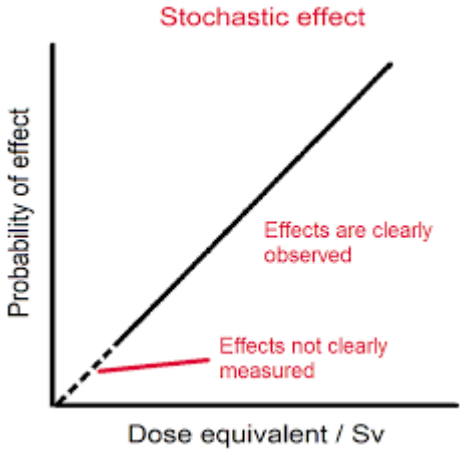

Figure 2.12: Relationship between probability of an effect and dose equivalent [13]

Examples of stochastic effects are:

- Radiation-induced cancer;
- Teratogenesis
- Heart disease.

- **Somatic Effects**

  Radiological effects on people are termed somatic effects. They result in cell damage which is passed on to successive generations of future cells, possibly leading to modification or impairment of both cells and tissues. Damage to cell membranes, mitochondria and cell nuclei result in abnormal cell functions, and affect cell division and growth, while accelerating their death. These effects include:

- Skin cancer;
- Cancer;
- Damage to the bone marrow;
- Radiation burns (Figure above 2.10)
- Damage to the lining of the gastro-intestinal tract.

According to the ICRP, the detriment of radiation exposure includes:

- The probability of inducing a fatal cancer;
- The chance of a non-fatal cancer occurring;
- The chance of severe hereditary effects; and
- The length of life lost if any of these above harm occurs [13].

- **Teratogenic Effects**

  Teratogenesis refers to a prenatal toxicity leading to structural or functional defects in the developing embryo or foetus. Teratogenic effects from exposure to radiation are believed to be a deterministic effect, with a threshold dose below which no such effect occurs. However, there are also stochastic effects affecting the unborn child, including carcinogenesis and mutagenesis, which have no threshold, and which are not classified as being teratogenic. According to the ICRP there are various risks and thresholds for prenatal exposure to radiation, at different stages of foetal development. These are summarized in Table 2.2.

Gestation Age	Stage	Potential Effect	Threshold	Risk
0 to 2 weeks	pre-implantation and implantation	Abortion	100-150 mSV	
3 to 8 weeks	organogenisis	Organ malformation	100-200mSv	
		Growth retardation (temporary)	100-250 mSv	
9 to 25 weeks	foetal	Mental impairment	100 mSv	
Whole pregnancy		Carcinogenesis	none	6 % / Sv
		Mutagenesis	none	1%/ Sv

Table 2.2: Effects of radiation exposure in utero

- **Genetic Effects**

Genetic effects occur when the DNA which encodes the genetic information is damaged, and the damaged genes and chromosomes are passed on from current to future generations. Genetic information is also contained in the chromosomes of germ cells, i.e the female ovum and male sperm [20].

2.6. Review of studies on radioactivity in soils

A background level of ionising radiation from natural sources has always existed on earth, and all living entities are inescapably exposed to it. Like fish in the sea, everything on earth is enclosed in a sea of radiation. Many radiological studies have been conducted over the past two decades, locally and internationally, and these have revealed the presence of uranium, thorium and potassium in anomalies in soil [21-37].

Some people live in areas with low or normal background radiation (mean effective dose less than 1.0 mSv y^{-1}) while others live in areas regarded as high background radiation areas. It is

however not desirable for human beings to live in high background radiation areas (mean annual effective dose equivalent greater than 1 mSv).

2.6.1. Local Studies on radioactivity in soils

In Namibia the natural radionuclides in various towns including Walvis Bay, Swakopmund, Wlotzkasbaken, Usakos, Karibib, Okahandja, Oshakati, Tsumeb, Rundu and Katima Mulilo have been studied [2, 4, 14, 25]. These studies have shown that the natural radioactivity may vary depending on the geological and geomorphological nature of the area studied.

For the town of Walvis Bay, the average activity concentrations of the radionuclides ranged from 14.5 to 27.2 Bq/kg for ^{283}U, 18.0 to39.7 Bq/kg for ^{232}Th and 363.2 to 586.9 Bq/kg for ^{40}K. The calculated average activity concentrations of ^{238}U, ^{232}Th and ^{40}K in the soil samples were 18.6 ± 4.6, 23.8 ± 8.4 and 460.3 ± 76.2 Bq/kg respectively. The values for ^{238}U and^{232}Th are below the worldwide mean values of 35 and 40 Bq/kg, respectively. However, the average activity concentration for ^{40}K is above the worldwide average of 400 Bq/kg. The measured annual dose rates for all samples gives rise to a mean value of 0.05 ± 0.01 mSv/y which is less than the maximum permissible limit of 1 mSv per year while the external hazard index has been found to be 0.24 ± 0.04. This result implies that the town of Walvis Bay has a normal background radiation. [2]

The average activity concentrations of ^{238}U, ^{232}Th and ^{40}K measured in soil samples from the Namibian coastal town of Swakopmund were found to be in the range of 34.9 – 68.1 Bq/kg, 55.0 -167.6 Bq/kg, and 572.0 – 747.3 Bq/kg, for the radionuclides ^{238}U, ^{232}Th and ^{40}K,

respectively. The mean activity concentration values for ^{238}U, ^{232}Th and ^{40}K were 46.4 ± 14.2, 91.1 ± 39.6 and 645.5 ± 69.5 Bq/kg, respectively. These average activity concentration values are well above the worldwide average values. However, the corresponding annual effective dose varies from 0.09 -0.20 mSv y^{-1} with a mean value of 0.13 ± 0.04 mSv y^{-1}, falling significantly within the range of the world wide average values [2].

For the settlement of Wlotzkasbaken, the measurements yielded activity concentration ranges of 51.52 to 104.1, 53.6 to 133.2 and 659.2 to 810.2 Bq/kg, for ^{238}U, ^{232}Th and ^{40}K, respectively. The mean activity concentration values for ^{238}U, ^{232}Th and ^{40}K were 69.6 ± 26.3, 79.5 ± 44.1 and 759.2 ± 68.4 Bq/kg, respectively. The corresponding annual effective dose varies from 0.10 -0.20 mSv y^{-1} with a mean value of 0.14 ± 0.05 mSv y^{-1}. The average activity concentrations of the radionuclides are higher than the world's average and this is a reflection of the fact that the settlement is in a uranium rich-region [2].

In the case of Usakos (also known by its Otjiherero name as Okanduu), the natural radioactivity levels of ^{238}U, ^{232}Th and ^{40}K measured in soil samples were found to have mean values of 44.2 ± 9.7, 74.8 ± 30.2 and 959.5 ± 194.7 Bq/kg, respectively. The measurements yielded activity concentration ranges of 33.1 to 52.9, 45.7 to 118.9 and 774.6 to 1336.5 Bq/kg, for ^{238}U, ^{232}Th and ^{40}K, respectively. The corresponding annual effective dose varies from 0.10 -0.18 mSv y^{-1} with a mean value of 0.13 ± 0.03 mSv y^{-1}. Similar to the town of Swakopmund and the settlement of Wlotzkasbaken, the average activity concentrations of the radionuclides found in the soil in Usakos are higher than the world's average and this is also a reflection of the fact that these towns are all in a uranium rich-region [2].

The results for the northern town of Oshakati were reported as varying from 6.7 to 12.9 Bq/ kg for ^{238}U, 5.2 to 12.8 Bq/kg for ^{232}Th and 36.8 to 119.8 Bq/kg for ^{40}K. The natural radioactivity levels of ^{238}U, ^{232}Th and ^{40}K measured in soil samples were found to have mean values of 9.5 ± 2.9, 8.2 ± 3.1 and 62.3 ± 28.9 Bq/kg, respectively. All these average activity concentrations were below the world's average and the implication thereof was that the town of Oshakati has a low background radioactivity and the concentrations of the natural radionuclides do not pose any significant radiological risks. The corresponding annual effective dose varies from 0.01 -0.02 mSv y^{-1} with a mean value of 0.01 ± 0.005 mSv y^{-1}, falling significantly within the range of the world wide average values [4].

The average activity concentrations of the radionuclides sampled from soil in Tsumeb ranged from 12.1 to 18.0 Bq/kg for ^{283}U, 21.3 to 31.2 Bq/kg for ^{232}Th and 296.5 to 488.4 Bq/kg for ^{40}K. The calculated average activity concentrations of ^{238}U, ^{232}Th and ^{40}K in the soil samples were 14.2 ± 3.3, 24.9 ± 6.1 and 380.1 ± 112.9 Bq/kg respectively. These values are below the worldwide mean values of 35, 40 and 400 Bq/kg, respectively. The measured annual dose rates for all samples gives rise to a mean value of 0.05 ± 0.01 mSv y^{-1} which is less than the maximum permissible limit of 1 mSv y^{-1} [4].

In the radionuclide study done for the town of Rundu, the average activity concentrations of the radionuclides sampled from soil in the town ranged from 5.8 to 9.0 Bq/kg for ^{283}U, 3.5 to 8.6 Bq/kg for ^{232}Th and 25.6 to 108.6 Bq/kg for ^{40}K. The calculated average activity concentrations of ^{238}U, ^{232}Th and ^{40}K in the soil samples were 7.5 ± 2.3, 5.8 ± 2.6 and 67.5 ±

45.6 Bq/kg respectively. These values are well below the worldwide mean values of 35, 40 and 400 Bq/kg, respectively. The measured annual dose for all samples gives rise to a mean value of 0.01 ± 0.005 mSv which is less than the maximum permissible limit of 1 mSv per year [4].

The results for the north-eastern town of Katima Mulilo were reported as varying from 6.0 to 15.9 Bq/ kg for ^{238}U, 1.9 to 14.1 Bq/kg for ^{232}Th and 21.2 to 89.8 Bq/kg for ^{40}K. The natural radioactivity levels of ^{238}U, ^{232}Th and ^{40}K measured in soil samples were found to have mean values of 9.4 ± 4.4, 6.4 ± 5.2 and 52.1 ± 28.7 Bq/kg, respectively. These average activity concentration values were below the world's average and this implies that the town also has a low background radioactivity and the concentrations of the natural radionuclides do not pose any significant radiological risks. The corresponding annual effective dose rate varies from 0.01 -0.02 mSv/yr with a mean value of 0.01 ± 0.007 mSv/yr, which falls within the range of the world wide average values [4].

The average activity concentrations of the radionuclides sampled from soil in Okahandja ranged from 25.9 to 71.7 Bq/kg for ^{283}U, 34.6 to 138.8 Bq/kg for ^{232}Th and 307.4 to 857.9 Bq/kg for ^{40}K. The calculated average activity concentrations of ^{238}U, ^{232}Th and ^{40}K in the soil samples were 40.9 ± 2.3, 57.9 ± 4.1 and 562.4 ± 24.5 Bq/kg respectively. These values are below the worldwide mean values of 35, 40 and 400 Bq/kg, respectively. The measured annual dose rates for all samples gives rise to a mean value of 0.10 ± 0.02 mSv/yr which is less than the maximum permissible limit of 1 mSv per year [14].

For the town of Karibib, which is situated in the Erongo region of Namibia, the measurements yielded activity concentration ranges of 14.3 to 43.1, 29.0 to 69.9 and 505.3 to 1168.4 Bq/kg, for ^{238}U, ^{232}Th and ^{40}K, respectively. The mean activity concentration values for ^{238}U, ^{232}Th and ^{40}K were 29.4 ± 2.1, 49.0 ± 3.9 and 824.3 ± 32.4 Bq/kg, respectively. The corresponding annual effective dose rate values yielded a mean value of 0.01 ± 0.01 mSv/yr. The average activity concentrations of the radionuclides are higher than the world's average and this is a reflection of the fact that the settlement is in a uranium rich-region [14].

From the studies conducted in various parts of Namibia, it is evident that radioactivity levels of the soil depend on geological aspects of the areas where they are found and this may vary from one place to another.

2.6.2. International Studies on radioactivity in soils

Natural environment radionuclides are responsible for the most of the external exposures of gamma radiation. This contribution is mainly due to the radionuclides of the natural series U-238, Ra-226, and Th-232, followed by K-40 and their decay products, universally present in the Earth [26]. Quantification and measurement of natural radioactivity content is thus very important as it helps to set a baseline level for future radiation impact assessment and for public and environmental protection purposes. It is for this reason that many studies have been done worldwide as part of the documentation of concentrations of natural radionuclides, particularly in the soil.

A study done in Iraq in 2016, to determine the levels of radioactivity in soil samples collected from different areas of Wassit governorate, showed that the average concentrations of ^{238}U, ^{232}Th, and ^{40}K are 19.4 ± 4.7 Bq/kg, 18.4 ± 5.05 Bq/kg, and 204.2 ±46.9 Bq/kg respectively, which is lower than the worldwide average value. While the average value of Radium equivalent, absorbed dose, indoor and outdoor annual effective dose, activity index, and internal and external hazard index for each sample have been found to be 85.182 Bq/kg, 39.962 nGy/h, 0.196 mSv/y, 0.049 mSv/y, 0.374, 0.313, 0.309, and 0.230 respectively, all of which are lower than the corresponding permissible limit value [27].

The activity concentrations of the natural radionuclides ^{238}U, ^{232}Th, ^{40}K and ^{137}Cs were measured in soil samples collected from different locations in Tulkarem district in West Back-Palestine in 2011 [28]. High-resolution gamma spectrometry (HPGe detector) was used to determine the activity concentration of these radionuclides in 72 surface soil samples taken

from areas in and surrounding Tulkarem city. The concentration of ^{238}U varied in the range 9.7 - 83.5 Bq/kg with an average value of 34.5 Bq/kg. The concentration of ^{232}Th varied in the range 5.3 - 44.8 Bq/kg with an average value of 23.8 Bq/kg. Additionally, for ^{40}K, the concentration values were in the range 10.2 - 404.0 Bq/kg, with an average value of 120.0 Bq/kg. Lastly, for ^{137}Cs the values were found in the range 1.0 - 24.5 Bq/kg with an average value of 7.8 Bq/kg. To assess the radiological hazard of the natural radioactivity, the absorbed dose rate (D*r*), the radium equivalent activity (Ra_{eq}), the effective dose rate (E*eff*), the annual effective dose equivalent (AEDE), Excess Lifetime Cancer Risk (ELCR), the radioactivity level index (Iγ), and the external (H_{ex}) and internal (H_{in}) hazard indices were calculated. The study concluded that there was no risk to the residents around Tulkarem city except some areas which had high concentration levels due to fallout ^{137}Cs. Hence, the probability of occurrence of any of the health effects of radiation is low and the measurements have been taken as representing baseline values of these radionuclides in the soil in studying area [28].

A study done in Egypt in 2013 to determine the radioactivity levels of soils sampled in Dakahlia, showed that there was enhanced levels of natural radioactivity and this correlated with the high values of Ra-226 [21]. Ra-226 is related to the external radiation hazard index and hence this information from the study in Egypt was an important alert for the local people to avoid the use of the soil for construction of dwellings.

Gamma-ray spectrometry of natural radioactivity was carried out in soil along the bank of river Kaduna Nigeria in 2013 [30]. The activity concentration in Bq/kg for ^{40}K and ^{232}Th were calculated from the % weight of ^{40}K and ^{232}Th determined in the soil samples. The mean

activity concentration of ^{40}K was found to be 1168.13 ± 94.67Bq/kg, with values ranging between 810.62 ± 21.91 to 1765.32 ± 31.30 Bq/kg. The mean activity concentration of ^{232}Th was found to be 18.76 ± 2.51Bq/kg, with values in the range of 8.12 ± 2.44 to 33.70 ± 6.90 Bq/kg. The mean activity concentration of ^{40}K found in the study area was higher than world average value while that of ^{232}Th is lower than the world average value [30].

In 2010, natural radioactivity analysis has been done for soil samples collected from different villages/towns of Hoshiarpur district of Punjab, India [31]. The measurements were done using an HPGe detector based on high-resolution gamma spectrometry system. The calculated activity concentration for ^{238}U, ^{232}Th and ^{40}K was found to vary from 8.89 to 56.71 Bq/kg, 137.32 to 334.47 Bq/kg and 823.62 to 1064.97 Bq/kg, respectively. This study found that the total average absorbed dose rate in the study area was 185.32 nGy/h. Calculations showed that the yielded value for average radium equivalent activity, 401.13 Bq/kg, was exceedingly higher than the recommended 370 Bq/kg. The calculated value of external hazard index (H_{ex}) was 1.097. Values calculated for Indoor and Outdoor annual effective doses varied from 0.61 to 1.28 mSv y^{-1} and from 0.15 to 0.32 mSv y^{-1}, respectively. A positive correlation, $R^2 = 0.71$ was observed between the concentration of ^{232}Th and ^{40}K [31].

A study to determine natural and artificial radioactivity in soil was conducted as part of a systematic study to provide a surface radiological map in Lebanon. Soil samples from the North Lebanon province were collected, measured and analysed. Two sets of independent High-purity Germanium (HPGe) detectors were used for the gamma-ray spectrometric measurement of the samples. These studies provided soil activity concentration levels for

primordial radionuclides, specifically members of the ^{238}U and ^{232}Th decay chains and ^{40}K. The ^{238}U and ^{232}Th radionuclides and ^{40}K activity concentration values ranged between 4 to 73 Bq/kg, 5 to 50 Bq/kg, and 57 to 554 Bq/kg, respectively. The study found the average values for ^{238}U, ^{232}Th and ^{40}K to be 27 Bq/kg, 24 Bq/kg, and 246 Bq/kg respectively. The calculated average specific activity concentrations of ^{238}U and ^{232}Th were comparable to the world average values reported in UNSCEAR (2000) of 35 Bq/kg and 40 Bq/kg respectively. The average specific activity concentration for ^{40}K was lower than the world wide average value of 400 Bq/kg. The measured annual dose rates for all samples gives rise to a mean value of 69 μSv/yr which is less than the maximum permissible limit of 1000 μSv per year [22].

In 2016, in the State of Kuwait, an evaluation of the radioactivity levels associated with naturally occurring radioactive materials was undertaken as part of a systematic study to provide a surface radiological map of the State. Soil samples from across Kuwait were collected, measured and analysed. Two independent High-purity Germanium (HPGe) detectors were used for the gamma-ray spectrometric measurement of the samples. These studies provided soil activity concentration levels for primordial radionuclides, specifically members of the ^{238}U and ^{232}Th decay chains and ^{40}K. The ^{238}U, ^{232}Th and ^{40}K radionuclides were found to have activity concentration values which ranged between 5.9 to 32.3 Bq/kg, 3.5 to 27.3 Bq/kg, and 74 to 698 Bq/kg, respectively. The calculated average specific activity concentrations of ^{238}U, ^{232}Th and ^{40}K in all the soil samples were 18, 15 and 385 Bq/kg respectively. These values are all below the worldwide mean values of 35, 40, and 400 Bq/kg, respectively. The measured annual dose rates for all samples gives rise to a mean value of 40.8 ± 3.0 μSv/yr which is less than the maximum permissible limit of 1 mSv per year while the

internal and external hazard indices have been found to be 0.23 ± 0.02 and 0.19 ± 0.01 respectively [32].

A similar study was conducted in Turkey's Aliaga-Foca industrial region. In the study, surface soil samples were collected and analysed for relevant radionuclides using a high sensitivity NaI(Tl) detector [24]. The natural radioactivity levels of ^{226}Ra, ^{232}Th and ^{40}K measured in these samples were found to be in the range of 14– 123 Bq/kg, 27-132 Bq/kg, and 141-1666 Bq/kg. The corresponding annual effective dose varies from 44 – 220 μSv/yr with a mean value of 106 μSv/yr, falling significantly within the range of the world wide average values.

In Cameroon, natural background dose measurements were conducted in the locality of Lolodorf, using a high-purity germanium detector. The mean activity concentrations of ^{226}Ra, ^{232}Th and ^{40}K were measured to be 329±491 Bq/kg, 414±309 Bq/kg and 2001±521 Bq/kg, respectively. The corresponding annual effective dose rates were determined to be 307 μSv/yr. The level of radioactivity for the study conducted in Cameroon is relatively high compared to the values reported for Turkey and Lebanon, however it is still within the world wide limit. The geological aspect of this study reported the presence of alkaline syenite. Syenite is a coarse-grained intrusive igneous rock of the same general composition as granite but with quartz either absent or present in relatively small amounts (<5%). Higher radiation levels are associated with igneous rocks such as granite, and lower sedimentary rocks. According to this study, granite rocks have been found to contain some amounts of U, Th and their decay daughter products. This study concluded that the specific levels are related to the types of rock from which the soils originate [33].

The natural radioactivity in soil in various areas of the Balachistan province of Pakistan was also measured in 2010. The mean activity concentrations of ^{226}Ra, ^{232}Th and ^{40}K were measured to be 21 Bq/kg, 30 Bq/kg and 454 Bq/kg, respectively. The corresponding annual effective dose equivalent was calculated to be 0.17 to 0.29 mSv/yr [34].

There are areas in the world which are known to have levels of exposure due to natural sources of radiation that are in excess of those considered to be "normal background". In 2011, a radiometric assessment around the Mrima Hill in Kenya was performed using a NaI(Tl) detector. The aim of this assessment was to determine the level of natural radioactivity due to naturally occurring radionuclides. The average concentrations of ^{238}U, ^{232}Th and ^{40}K were 207.0 ± 11.3 Bq/kg, 500.7 ± 20.0 Bq/kg and 805.4 ± 20.0 Bq/kg, respectively. The mean absorbed dose rate in air was found to be 440.7 ± 16.8 nGy/h and the annual average effective dose was 1.11 ± 0.01 mSv y^{-1}, which shows that the area has elevated levels of radioactivity as it is higher than the recommended value of 1 mSv y^{-1} [35].

Humans are always exposed to a background radiation spread of radioactive nuclei in the environment, particularly, in soil. The amount of background radiation is different in terms of height, the amount of the nuclei present in the soil, and the geographical conditions of different regions. The concentration of radioactive isotopes in soil is an indicator of radioactive accumulation in the environment, which impacts humans, plants, and animals. They are typically long lived, with half-lives often about hundreds of millions of years. As observed from the studies described above, it is evident that natural environmental radioactivity due to gamma radiation may depend primarily on geological and geographical conditions, and appear

at different levels in the soils of each region in the world [21 - 37]. It is important that the natural radioactivity, which exists in the soil, must be investigated to determine the population's exposure to radiation.

The natural radioactivity in a number of towns and industries has been studied in Namibia, however there are still some towns that are yet to be studied. A major gap in the national related studies is that not much attention has been given to investigating the behaviour of the radionuclides in the environment and their transfer to humans through ecological and food chains.

3. Chapter 3: Research Method and Experimental Set-up

This section will discuss the study area in terms of geology, topography and a general background description of the area. Thereafter, the experimental set up and various components of the HPGe detector used will be discussed. The performance characteristics of the detector will also be presented. This will be followed by a discussion on the actual sample collection and sample preparation. The process/procedure followed in taking measurements will be described, including detection and counting of radiation. Finally, the radiological parameters calculated and the formulas used will be discussed.

3.1. Study Area

The town of Omaruru is named after a word in Otjiherero translated as ‘bitter milk’ given the history of cattle that used to browse on a local bush which turned their milk bitter. Omaruru has since the year it was established in 1863 remained an important contributor to the country’s economy due to its strategic location and economic potential surrounding the area. Omaruru town has an area of 352 square kilometers and is situated near one of Namibia's most popular tourist drawcards, the volcanic formed Mount Erongo (situated 40 kilometers west of Omaruru) measuring 2,350 meters above sea level and the only place on Earth where the dung beetle species called Versicorpus erongoensis could be found. The town borders Karibib in the south western direction and Otjozondjupa region in the North eastern direction. Its location connects the coastal towns (Swakopmund, Walvis Bay and Henties Bay) to the central and northern parts of the country which makes it a gateway town to the northern part of the country. Omaruru is located 240 kilometers away from Windhoek the capital city of the country, as shown in Figure 3.1 and Figure 3.2, and is situated on the usually dry Omaruru river, which is a source of underground water supplied to the town and nearby places.

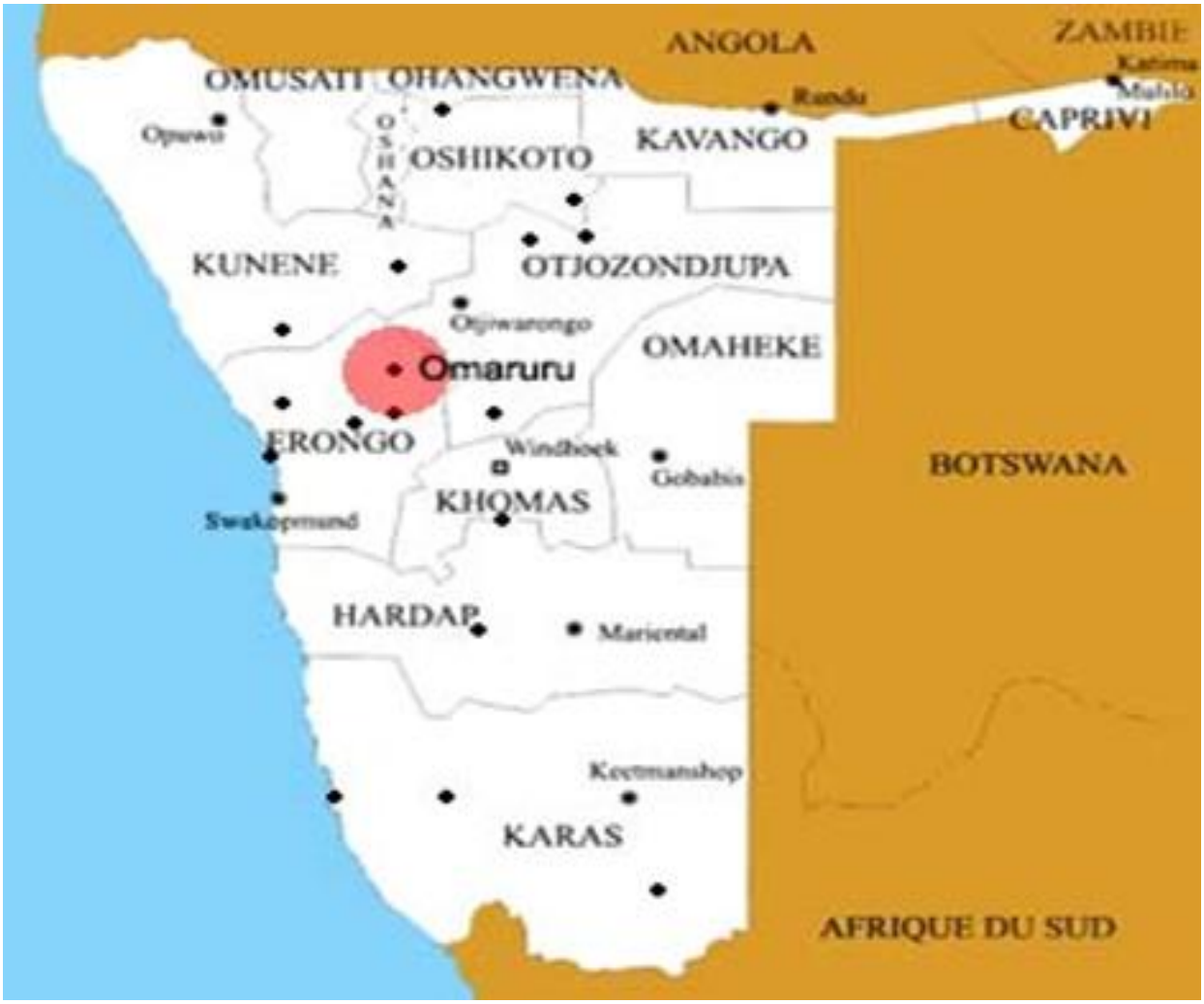

Figure 3.1. Map of Namibia [38]

Figure 3.2. Map showing Omaruru and Neighbouring towns [38]

The geological material typically found in Omaruru is part of the Damara orogeny, as shown in Figure 3.3. The geodynamic evolution of the late-Proterozoic Pan African Damara orogen was accompanied by magmatic activity of essentially granitic character. Broad swarms of zoned and unzoned pegmatites with contained U, Sn, and rare-metal deposits are associated with the late- to post-tectonic stages of granite intrusion (Sn-W metallogeny in the Damara orogen, South West Africa/Namibia). The Fundamental Complex is exposed over enormous areas throughout the whole of South West Africa. It consists of ancient gneissoid and granitic rocks, schists, quartzites, crystalline limestones, and other more or less metamorphosed sediments. The task of unravelling the stratigraphical succession of its sedimentary components presents great difficulties, but they are also usually so completely interfolded that unconformities, which no doubt exist, have to a large extent been obliterated. Investigations in the region between the Khan and Swakop rivers have proved the existence of at least two groups of ancient rocks: an older one, the Abbabis system, separated by an unconformity from a younger group, known as the Damara system. In the area

under discussion the ancient rocks appear to belong mostly to the Damara system,{i) though the possibility of members of the Abbabis system occurring interfolded with the latter cannot be discarded, since similar rock-types are found in both groups [8].

In this area a great thickness of mica schists forms the highest represented group of the Damara system, and is followed in descending order by the Marble series. The Quartzite series, which is the lowest member of the Damara system, does not occur anywhere in the area, its stratigraphical place being taken by mica schists and greywackes underlying the marble horizon.

The dominant soil type in Omaruru is Eutric Regosol, as shown in Figure 3.4. Eutric means ‘fertile soils with high base saturation’ and Regosol are ‘soils with medium to fine textured of actively eroding land scapes’.

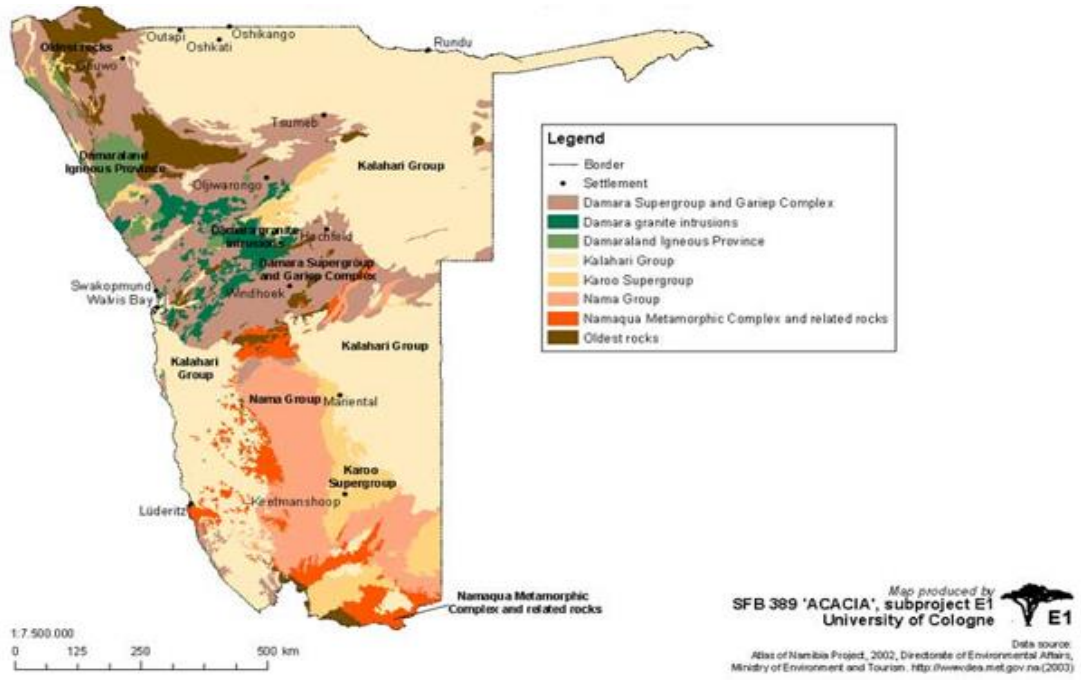

Figure 3.3 Geology of Namibia [39].

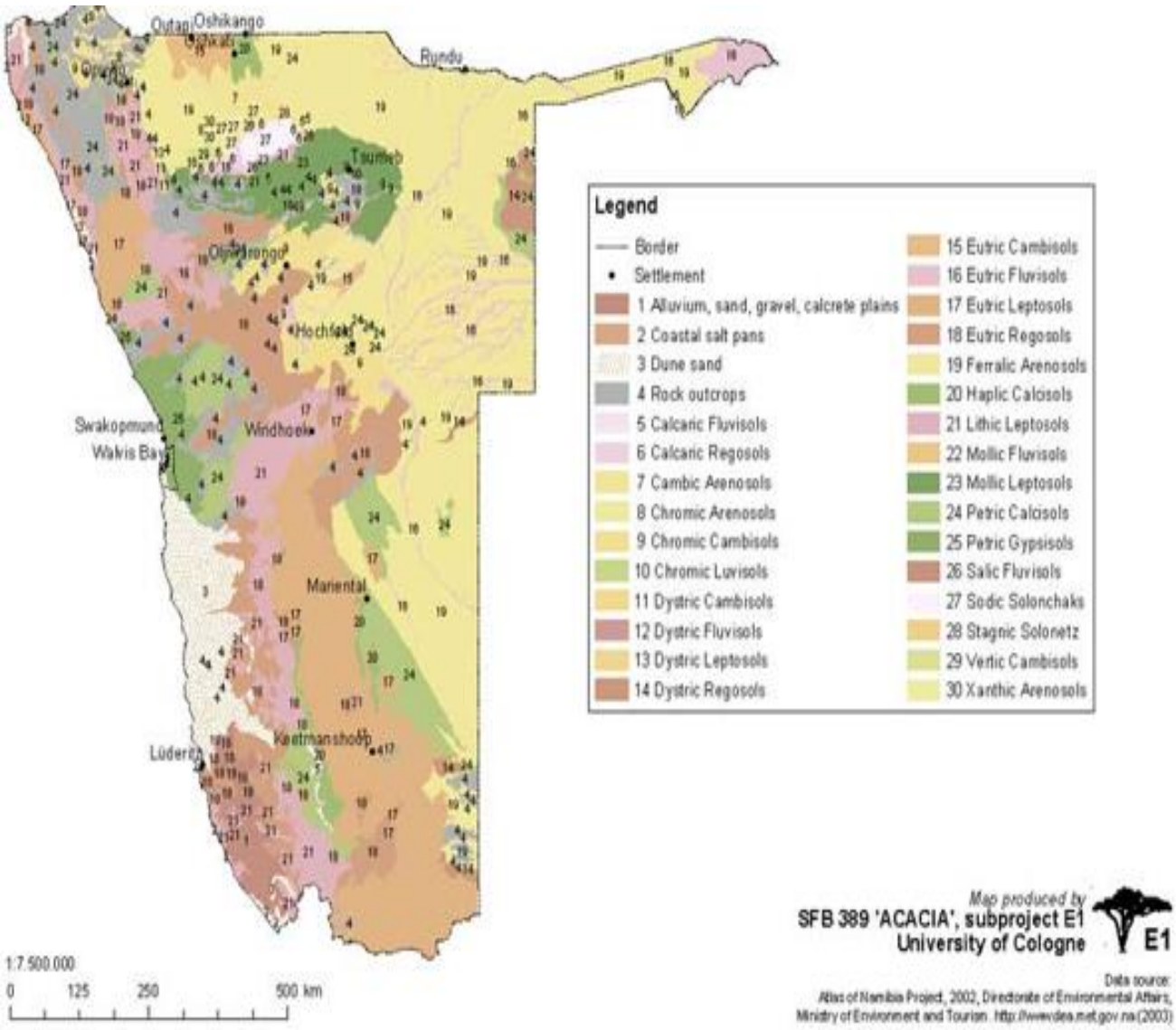

Figure 3.4 Dominant soils in Namibia [40]

3.2 Experimental Set-Up

The HPGe technique and Windows method was used for measuring primordial radionuclide activity concentration in soil samples [42].

3.2.1. HPGe Gamma Spectrometer

In this study a high purity germanium (HPGe) detector was used to determine the concentrations of gamma emitting radionuclides, in the nuclear physics laboratory in the department of Physics at the University of Namibia. The system is a Canberra semiconductor (HPGe) spectrometer with Genie 2000 software for quantitative analysis of the radionuclides. High resolution gamma spectroscopy provides fast, accurate and non-destructive analysis of natural radionuclides in environmental samples. The operation of this detector involves the following: first, the photon energy is completely or partly converted into kinetic energy of electrons (and positrons) by *photoelectric absorption*, *Compton scattering* or *pair production;* second, the production of electron-hole pairs; third, the collection and measurement of charge carriers.

The equipment in the laboratory included an HPGe detector, lead (Pb) shielding, PC based data acquisition system, digital weighing balance, and standard reference materials. The results obtained enable an estimation of the health hazard indices by gamma-emitting radionuclides.

3.2.2. Physical layout

Figure 3.5 – Figure 3.9. shows experimental set up used in the present study (the picture was taken in the Radiation Laboratory at the University of Namibia.

The lead castle, which opens from the top, shields the detector; and the dewar is for holding liquid nitrogen (LN_2). The oscilloscope is used to set and monitor the pulse properties while the NIM crate carries the amplifier. After amplification the signal is processed in the MCA card in the PC, and then displayed to the desktop [10].

All radioactive sources are kept in a metal safe far away from the set up (approximately 5 meters) in order to avoid the contribution of such sources to the background during counting. The laboratory has an air conditioning facility that ensures the maintenance of the normal temperatures around 18 °C.

3.2.3. Lead Castle

Lead is the material employed in the shielding of the detector used in this study. It makes a good shielding material due to its high density and large atomic number. A standard 25% (relative efficiency) detector measurement in a 10 cm thick lead shield will reduce the environmental background by a factor of 1000; thus enabling one to measure $1000 \approx 30$ times weaker sources with the same statistical accuracy [10].

In this study a 10 cm thick lead castle was used. The inside of the castle was lined with a copper layer of 1.5 mm thickness and 1.0 mm tin lining with an outer jacket of 9.5 mm thick low carbon steel . The copper layer is there to attenuate the X-rays from the lead (as shown in Figure 3.5.). A typical background spectrum measured with the HPGe is shown in Appendix E.

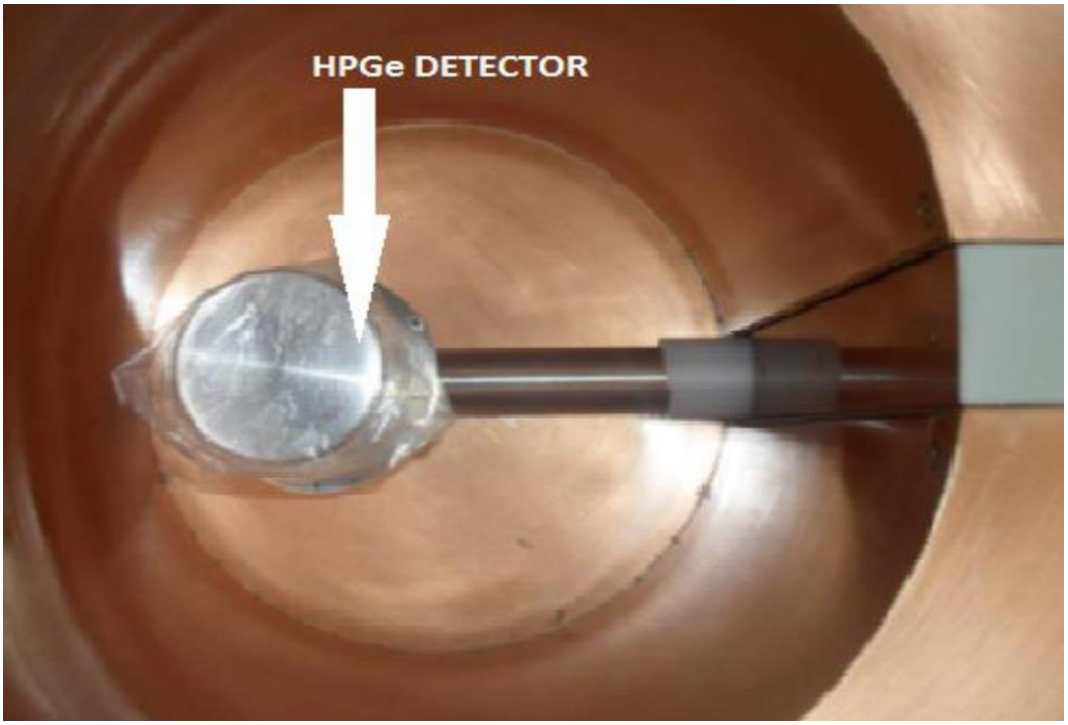

Figure 3.5. The HPGe detector in a Lead shield [14]

Figure 3.6. HPGe Detector with empty bottle ready for background counting [14]

3.2.4. HPGe technical specifications

The High-purity germanium detector (HPGe) used in this study is basically a cylindrical germanium crystal with an n-type contact on the outer surface, and a p-type contact on the surface of an axial well. The germanium crystal is located inside the lead shield. The HPGe coaxial detector used had a measured energy resolution of 1.0 keV FWHM at 1.22 keV and 1.9 keV FWHM at 1332 keV, with 25% relative efficiency (Canberra model GC2519). The detector was placed inside a Canberra Model 737 lead shield having a thickness of 10 cm. In addition, it had a graded 1.5 mm copper and 1.0 mm tin lining with an outer jacket of 9.5 mm thick low carbon steel [14].

3.2.5. Electronics

The electronic system for this semiconductor detector (HPGe) is shown schematically in Figure 3.7. The system also consists of a Model 2100 Bin/Power Supply providing mounting space for a Model 1786 LN_2 monitor and a High Voltage Power Supply (HVPS) Model 9645. It also includes a Model 9660 Digital Signal Processor (housing a Model 2016 Amplifier-TCA, an Analog to Digital Converter (ADC)), an Acquisition Interface Module (AIM 556A) Multichannel Analyser (MCA). A Genie® 2000 software (version 2.0) was used to analyse the spectra acquired in the measurements.

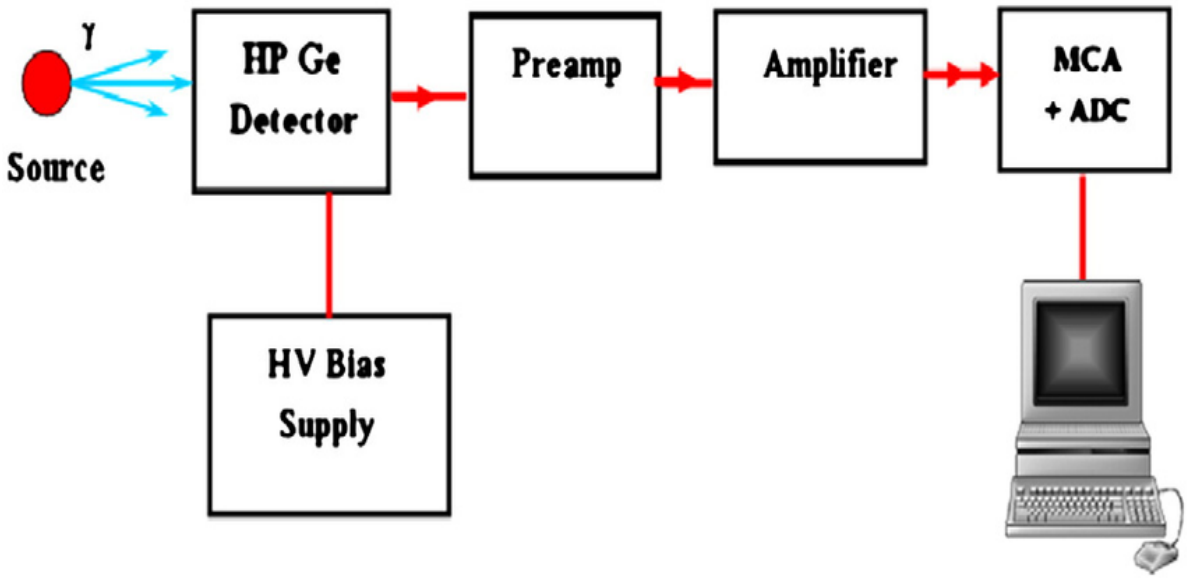

Figure 3.7. Block diagram of a typical gamma spectroscopy system [41]

HPGe detectors are operated at temperatures of around 77 K, in order to reduce noise from electrons which may be thermally excited across the small band gap at standard temperatures. There are weekly fillings of the HPGe liquid nitrogen dewar (capacity of about 20 liters) to provide for such low temperatures. Figure 3.8. shows a cross sectional diagram of a germanium detector.

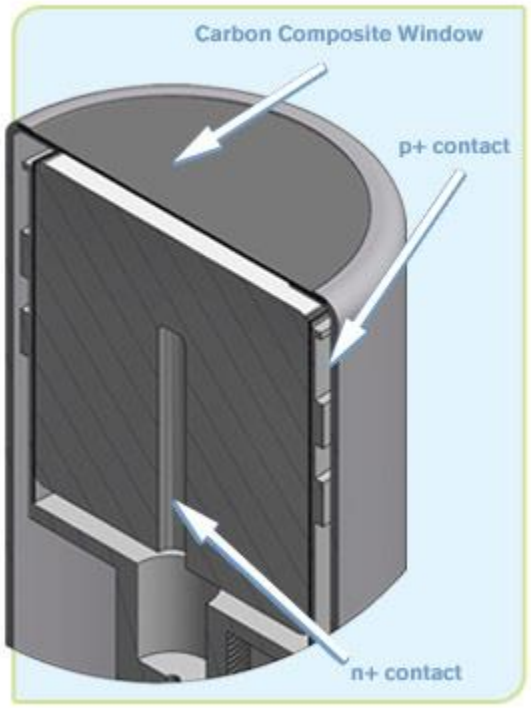

Figure 3.8. Cross section view of n and p type HPGe Detector [14]

3.2.6. Figure of merit

To keep track of the performance and reliability of the detector it is imperative to keep on checking our results based on the detector specifications. This is achieved by doing the energy calibration, checking the Full Width at Half Maximum (FWHM), and determining the peak to Compton ratio. The background measurements were done in each case to ensure derivation of proper concentrations.

3.2.7. Energy calibration

Prior to acquisition of the data, energy calibration has to be performed as part of the setting up procedure. Identifying the gamma rays within a measured spectrum requires matching the energies of the gamma rays with those emitted by known radionuclides. The energy calibration of the detector system used in this study was done by measuring mixed standard point sources of known radionuclides with well-defined energies within the energy range of interest. In the calibration: ^{22}Na, ^{60}Co and ^{137}Cs point sources were used. Energy calibration was done to obtain a relationship between the peak position in the spectrum and the corresponding gamma-ray energy as shown in Table 3.1. The spectrum of the gamma-ray emitting sources with known specific energy values was acquired long enough to identify the peak energies in the spectra. These point sources were selected to cover a wide energy range over which the spectrometer is to be used. The process involved measuring the spectrum of the point sources (of precisely known energies) and comparing the measured peak position with energy. This involves marking the peaks in the acquired spectrum with their true energies, then using the Genie 2000 software calibration analysis functions to fit the linearity graph as shown in Figure 3.9. The system was also calibrated using standard reference materials provided by the IAEA namely RGU-1, RGTh-1 and RGK-1. Figure 3.10. is a photograph of the reference materials. The spectra obtained for these reference materials are shown in Figures 3.11 (a), (b) and (c). With this information stored in the memory of the MCA, radionuclides present in the soil samples could easily be identified by comparing their spectra with those of the reference materials.

Any source whose peaks are known can be used to do the energy calibration. In our study sources ^{40}K, ^{232}Th and ^{238}U sources were also often used. The energies of prominent γ-ray lines are presented in Table 3.2 below.

The spectrum has to be measured for long enough time in order to determine the peak properties with sufficient accuracy for the peaks to be used for the calibration. The calibration process involves marking the peaks to be used and their true energy.

Radionuclide	**Peak Energy (keV)**
^{137}Cs	661.66
^{60}Co	1173.24 and 1332.50
^{22}Na	1274.54

Table 3.1 Point sources used for energy calibration

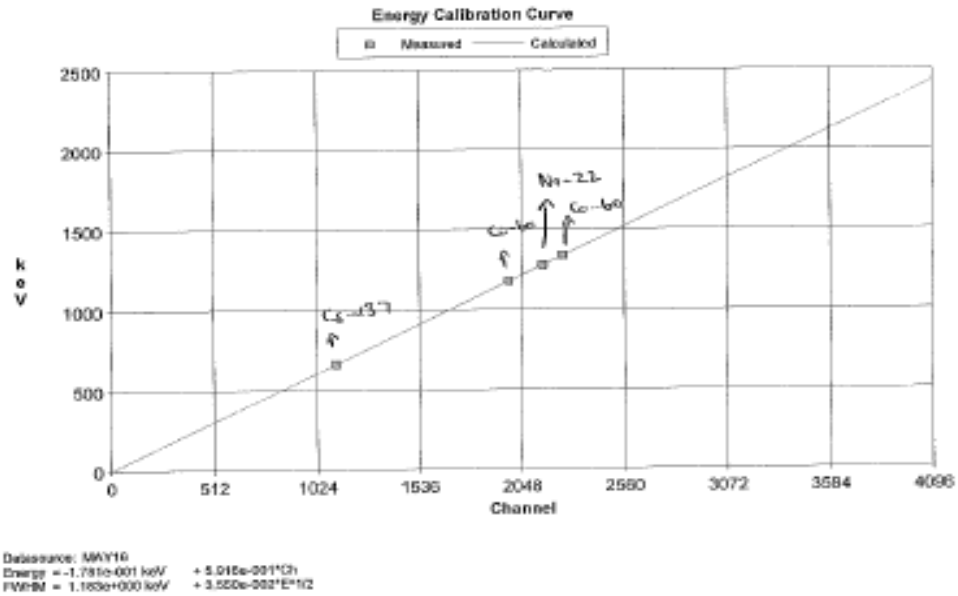

Figure 3.9: Energy Calibration Curve

Decay Series	**Decaying nucleus**	**Energy (keV)**	**FWHM (keV)**
^{238}U	$^{226}Ra/^{235}U$	186.1	1.51
^{232}U	^{212}Pb	238.6	1.54
^{238}U	^{214}Pb	295.1	1.57
^{232}Th	^{228}Ac	338.4	1.60
^{238}U	^{214}Pb	352.0	1.60
^{232}Th	^{208}Tl	583.0	1.73
^{238}U	^{214}Bi	609.3	1.74
^{232}Th	^{212}Pb	727.3	1.81
^{232}Th	^{228}Ac	911.2	1.91
^{238}U	^{214}Bi	1120.3	2.03
^{40}K	^{40}K	1460.8	2.21
^{238}U	^{214}Bi	1764.5	2.38
^{238}U	^{214}Bi	2204.1	2.62
^{232}Th	^{208}Tl	2614.4	2.85

Table 3.2: γ-ray energies with associated Full Width at Half Maxima (FWHM) for γ-ray lines associated with decay of ^{40}K and the series of ^{238}U, ^{232}Th [10]

Figure 3.10. Reference materials used [14].

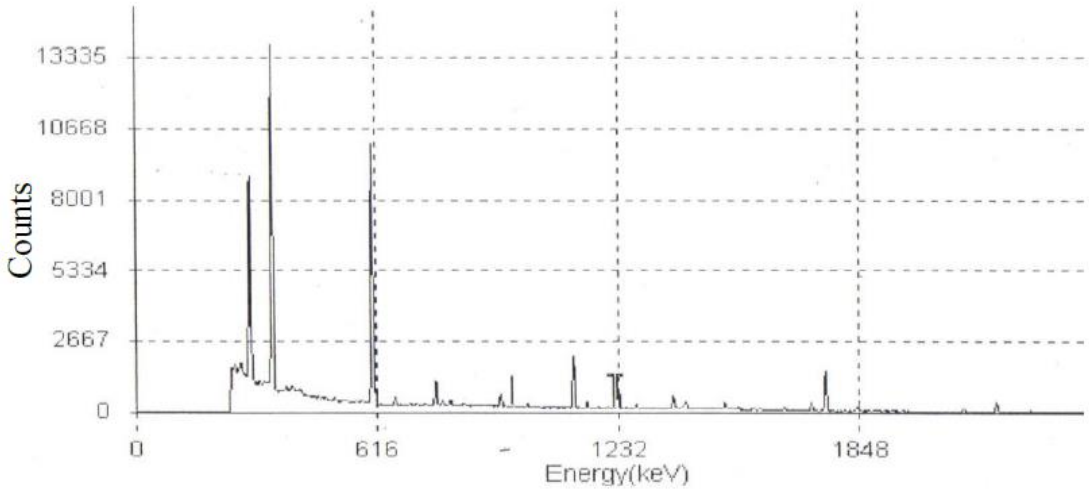

(a)

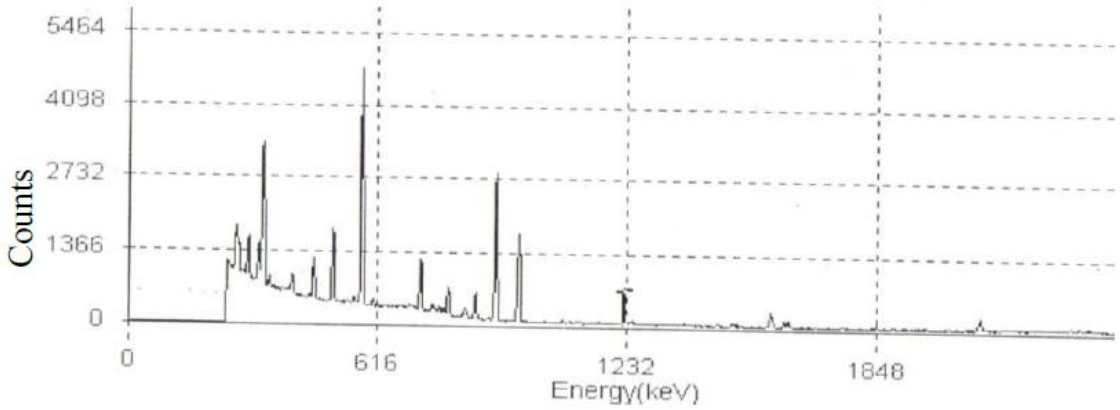

(b)

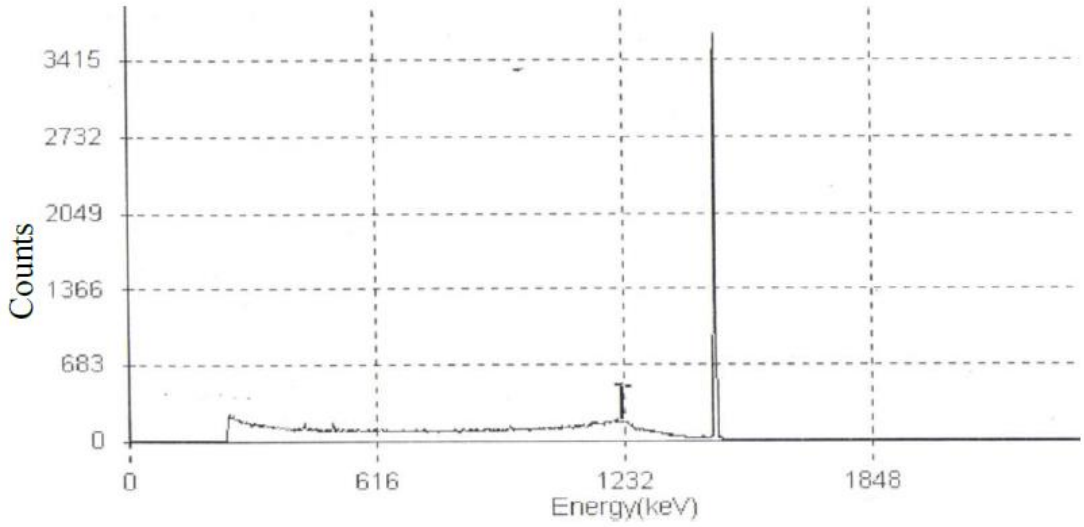

(c)

Figure 3.11: Spectrum of (a) RGU-1, (b) RGTh-1 and (c) RGK-1 reference materials.

3.2.8. Energy resolution

The energy resolution of the HPGe detector system as a function of γ-ray energy was calculated after the energy calibration. The energy resolution of the detector (at a particular γ-ray energy) is conventionally defined as the full width-to-half maximum (FWHM) of the peak divided by the

peak energy, that is the width of a gamma ray peak at half of the highest point of the peak. Therefore, the energy resolution, which is a dimensionless fraction, is conventionally expressed in percentages. Small percentage resolution of a peak implies good resolution. This is the most common property of a spectroscopic system that expresses a detector's resolution.

In principle one should be able to resolve peaks at two energies, which are separated by more than one value of the detector FWHM at that energy. In order to parameterize the dependence of FWHM on γ-ray energy, the FWHM data for the lines given in Table 3.2 were fitted using a linear function. The fit to the data are shown in Figure 3.12 The results for the FWHM calibration shown in the Table 3.2, were obtained from the following equation:

$$FWHM = AE + B$$

where A and B are constants deduced by the software program and E is the γ-ray energy. The graph in Figure 3.12 was then plotted from these results

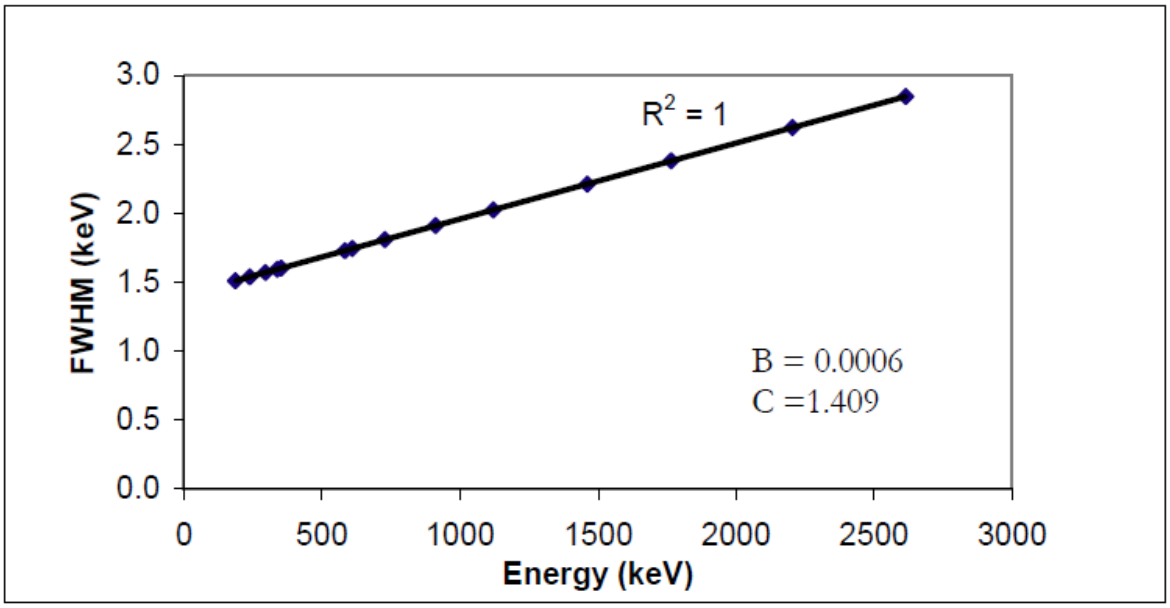

Figure 3.12. A Full Width at Half Maximum calibration graph with a line of best fit [10].

The resolution of the detector system used in this study as mentioned earlier is 1.0 keV FWHM at 122 keV and 1.9 keV FWHM at 1332 keV. In relative terms this translates to the FWHM (in keV) divided by the energy of the gamma ray and multiplied by 100. Hence, in relative terms, the resolution of the detector system used is 0.82% at 122 keV and 0.14 % at 1332 keV. This indicates that the system has a high resolution. Figure 3.13 shows the resolution of a gamma ray spectrometer.

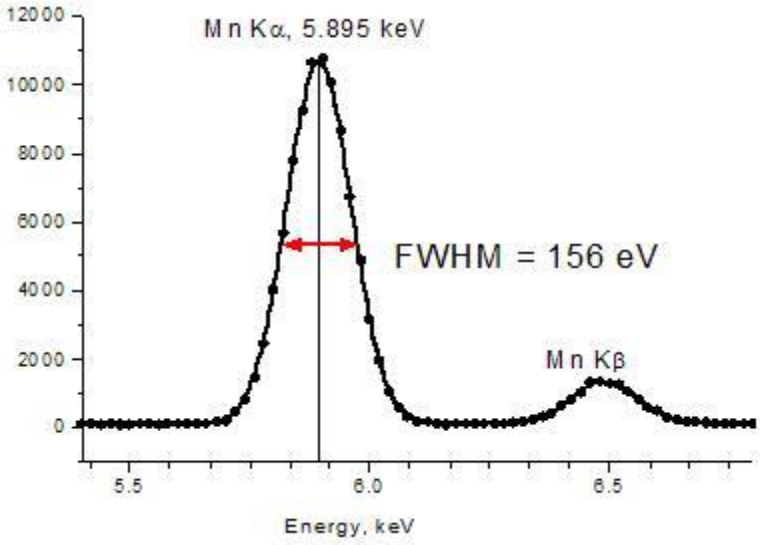

Figure 3.13: Diagram illustrating the energy resolution of a gamma ray spectrometer. The spectrometer energy resolution is defined as the full width of a photopeak at half the maximum amplitude (FWHM) [43].

3.2.9. Peak to Compton Ratio

The Peak-to-Compton ratio is an important quantity defined as the ratio of the counts in the channel corresponding to the highest number of counts per channel in the photo-peak (photopeak centroid) to the counts in the 'typical channel' of the Compton continuum. This 'typical channel' is defined as the region of interest between 1040-1094 keV for a ^{60}Co source. The Compton continuum results

from the Compton scattering in which the gamma rays entering the detector will not deposit their full energy on interaction with matter. This partial energy event appears in the spectrum as an event below the full energy peak in the Compton continuum. The Peak-to-Compton ratio ranges from 30 to 60 for coaxial germanium detectors when using the 1332 keV line associated with the ^{60}Co decay [10].

3.3. Sample Collection and Sample Preparation

A total of 50 samples, weighing about 1 kg each, was collected from 10 geographical areas (shown in Figure 3.14. in the town of Omaruru. Soil samples were collected from undisturbed areas with a natural morphology. All the sites chosen were away from roads, buildings, railway lines, industrial or agricultural sites and rivers. A 1.0 m^2 area was chosen and samples were taken by first clearing vegetation and other organic matter from the surface. The samples were collected at a depth of about 2cm - 5cm below the soil surface as shown in Figure 3.15 (a) Gloves, dust masks, spades and digging equipment were employed to collect the samples. They were then placed in labelled nylon plastic bags corresponding to the areas and sites where they were collected. All samples were then transported from the site(s) to the Laboratory in Windhoek for processing.

At the laboratory, the samples were left to dry at room temperature under normal laboratory conditions for about 72 hours as shown in Figure 3.17. After removing stone, vegetation and organic matter the dried soil samples were pulverised and sieved through a 2 mm mesh screen as shown in Figure 3.18. 500 g of each sample were carefully weighed and placed in 500 ml polythene bottle similar to those of the reference materials as shown in Figure 3.10. Before measurements using the gamma spectrometry detector system, the air tight bottles were stored for about four weeks in order to reach radioactive equilibrium between ^{226}Ra and ^{232}Th and their progeny.

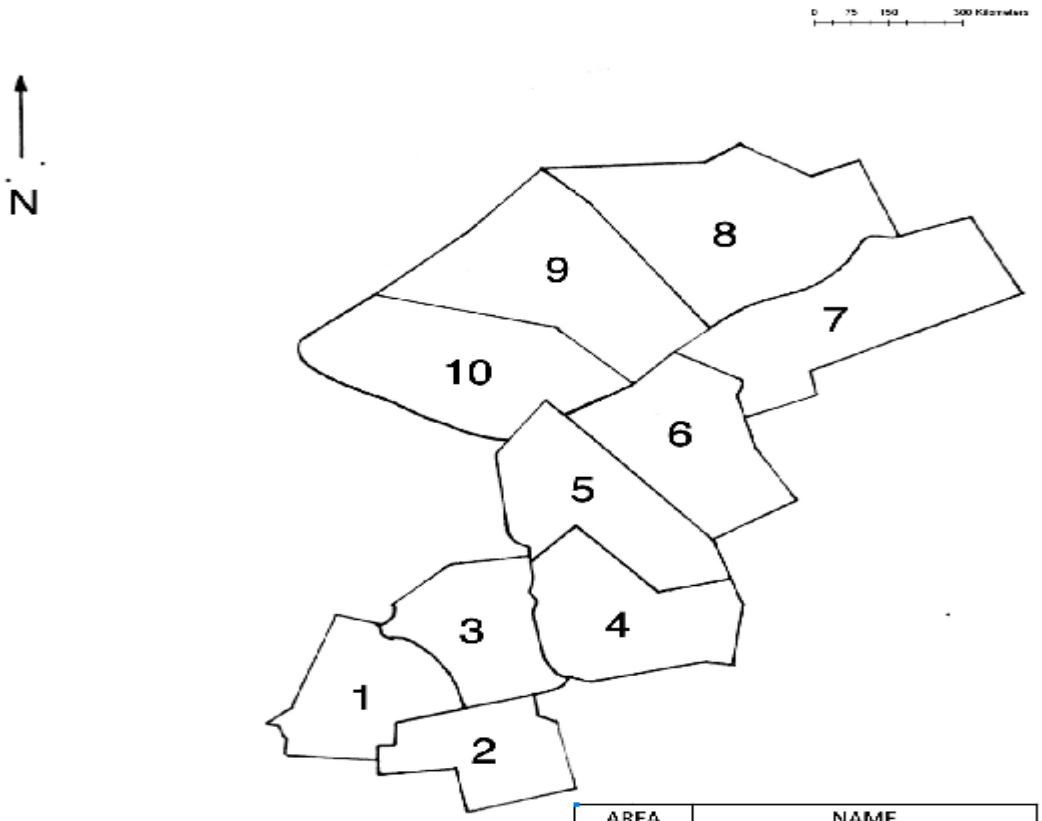

AREA		NAME
1	HA	Hakahana 1 (HA)
2	HB	Hakahana 2 (HB)
3	OA	Ozondje 1 (OA)
4	OB	Ozondje 2 (OB)
5	OC	Ozondje 3 (OC)
6	OS	Proposed Olympic Stadium (OS)
7	RS	River Side (RS)
8	MP	Municipality (MP)
9	PS	Omaruru Primary School (PS)
10	ID	Industrial Area (ID)

Figure 3.14. The 10 geographical areas sampled in the town of Omaruru.

Figure 3.15 a) Sample collection

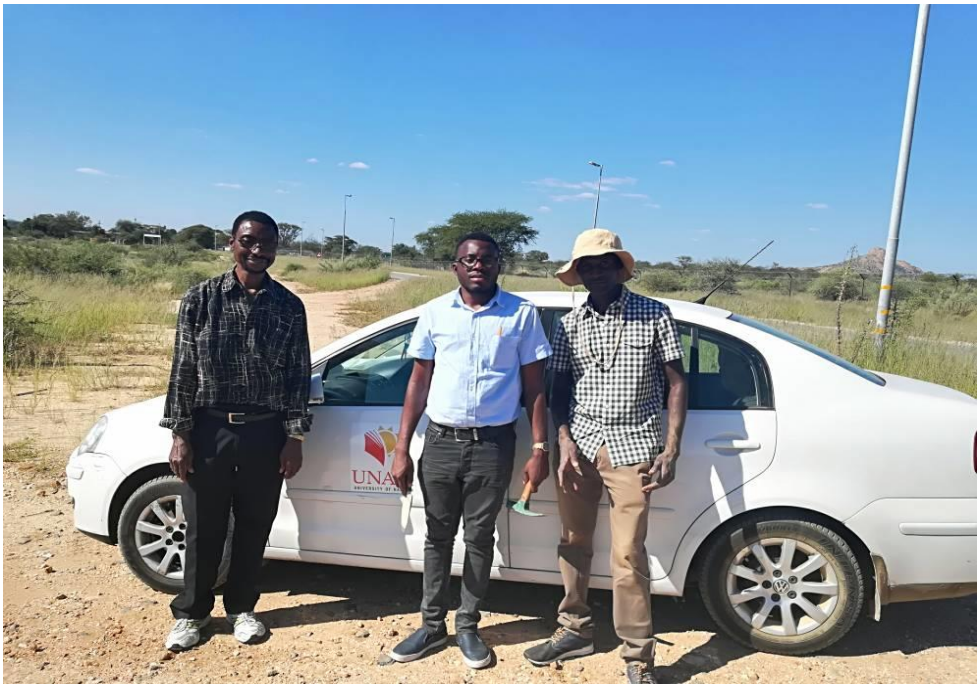

Figure 3.15 b) UNAM staff and volunteer that were part of sample collection. From left to right, Prof. J.A Oyedele, Mr. E. Taapopi and a local assistant.

Figure 3.16. Determination of the weight of a soil sample using an electronic scale.

Figure 3.17 Drying of soil samples

Figure 3.18 Preparation of soil samples

3.4. Procedure and Measurement

The background radiation around the detector was counted for 10800 seconds (3 hours) as well as 43200 seconds (12 hours) with an empty polythene bottle having the same dimensions as the soil samples. As discussed earlier, a well-shielded detector was used in the study and the background spectrum was stored in the MCA. The background radiation was low and there were no peaks at the channels corresponding to the peaks of interest or of the reference materials.

To reduce the contribution from background radiation in the laboratory, the samples were kept in a lead shield having a shielding efficiency of 95 %, while recording the spectrum [44].

3.5.Radiological parameters

In order to know the radiological effect in the study area, different radiological parameters and indices were calculated and the details of the calculations are presented in Table 3.3.

3.5.1 **Activity Concentration (C)**

All the elements of radioactive chains are influential on late balance, thus making it possible to calculate the concentration of an element in the series in terms of another one's concentration [14]. The number of counts obtained under a photo peak in a spectrum is related to the activity concentration of the radionuclide producing the peak in the soil. For the primordial radionuclides ^{40}K, ^{232}Th and ^{238}U in the soil samples, the activity concentrations were calculated from the corresponding photo peaks in the spectra. The activity concentration of ^{238}U was evaluated from the intensity of 609 keV gamma transition line of ^{214}Bi, while the activity concentration of ^{232}Th was determined using the 911 keV gamma line of ^{228}Ac. The 1460.75 keV gamma ray of ^{40}K was used to determine the activity concentrations of the ^{40}K. The net peak area A is proportional to specific activity concentration C of the radionuclide [14].

That is,

$A \propto C$

or

$A = kC$

therefore

$k = A/C$……3.1

where k is a constant for a given element

Therefore, for a given element X (e.g. ^{232}Th) in a standard source

$$k_{standard}^{X} = \frac{A_{standard}^{X}}{C_{standard}^{X}} \quad \ldots\ldots 3.2$$

Similarly, for element X (e.g. ^{238}U), in the sample

$$k_{sample}^{X} = \frac{A_{sample}^{X}}{C_{sample}^{X}} \quad \ldots\ldots 3.3$$

rearranging equation 3.3

$$C_{sample}^{X} = \frac{A_{sample}^{X}}{k_{sample}^{X}}$$

Since $k_{standard}^{X} \equiv k_{sample}^{X}$ for a given element X, therefore

$$C_{sample}^{X} = \frac{A_{sample}^{X}}{k_{standard}^{X}} \quad \ldots\ldots 3.4$$

3.5.2 **Absorbed Dose Rate (D)**

The quantity used to measure the "amount" of ionizing radiation is the absorbed dose, or simply known as dose. The absorbed dose rate is determined from the activity concentrations of the radionuclides ^{40}K, ^{232}Th and ^{238}U in the soil. The UNSCEAR 2000 report provides guidelines on how to calculate the Absorbed Dose Rate (D) due to gamma radiation in air at 1m above the ground [40]. In this study the absorbed dose rate (D) was calculated using the formula.

$$D(nGy/h) = 0.462C_U + 0.604C_{Th} + 0.0417C_K \quad \ldots\ldots 3.2$$

where C_U, C_{Th}, C_K are the activity concentrations of ^{238}U, ^{232}Th and ^{40}K respectively in the sample.

3.5.3 **Annual Effective Dose Equivalent (AEDE)**

To estimate the annual effective dose, the conversion coefficient from absorbed dose in air to effective dose (0.7 Sv Gy^{-1}) and an outdoor occupancy factor (0.2) proposed by UNSCEAR 2000 are used [42]. That is, the annual effective dose rate (in mSv y^{-1}) was calculated using the formula,

$$Effective\ DoseRate\ (mSv/yr) = (nGy/hr) \times 8760\ (hr/yr) \times 0.7 \times (10^3 mSv/10^9)\ \eta Gy \times 0.2 \ldots..3.3$$

3.5.4 **Radium equivalent (Ra_{eq})**

The Radium equivalent activity is a radiological index that represents the activity levels of ^{238}U, ^{232}Th and ^{40}K as a single quantity, it takes into account the radiation hazards associated with each component. The recommended maximum value of Radium equivalent activity is 370 Bq/kg [14]. The Radium equivalent activity (Ra_{eq}) is given by the expression

$$Ra_{eq} = C_U + 1.43C_{Th} + 0.077C_K \ldots\ldots\ldots\ldots\ldots\ldots\ldots\ldots\ldots\ldots\ldots\ldots\ldots\ldots\ldots\ldots\ldots\ldots 3.4$$

where C_U, C_{Th} and C_K are the activity concentrations of ^{238}U, ^{232}Th and ^{40}K respectively.

A computer program was written in Python language to calculate all the above parameters (in equations 3.2, 3.3 and 3.4).

3.5.5 **Hazard Index (H_{ex})**

A widely used hazard index (reflecting external exposure) called the external hazard index, H_{ex}, is defined as

$$H_{ex} = 370C_U + 259C_{Th} + 4810C_K \ldots\ldots\ldots\ldots\ldots\ldots\ldots\ldots\ldots\ldots\ldots\ldots\ldots\ldots\ldots\ldots\ldots\ldots 3.5$$

The value of the index (H_{ex}) must be less than unity for the radiation hazard to be negligible [42].

4. Chapter 4: Results and Discussion

4.0. Introduction

In this chapter, the results of the measurements of natural radioactivity in the soil samples analysed from Omaruru are presented and discussed. A comparison/correlation analysis will also be done between the values obtained for the different radionuclide concentrations.

4.1 Natural radioactivity in Omaruru

4.1.1 Radionuclide concentrations in Omaruru

The ten geographical areas from which soil samples were collected in the town of Omaruru are shown in Figure 3.14 and the concentrations of ^{238}U, ^{232}Th and ^{40}K measured in each of the 50 soil samples collected from the town are shown in Appendix A. The mean activity concentrations of ^{238}U, ^{232}Th and ^{40}K in the soil samples collected from each of the ten geographical areas of Omaruru are shown in Table 4.1 and Figure 4.1. As could be observed in the Table 4.1 and Figure 4.1, the activity concentration of ^{238}U is highest in the OC area with an average of 89.3 ± 21.8 Bq/kg and varies from (58.4 to 111.1 Bq/kg) but lowest in the PS area with an average of 48.6 ± 4.8 Bq/kg (and varies from 43.0 to 56.3 Bq/kg). The mean activity concentration of ^{238}U from all the soil samples across the town of Omaruru is 63.9 ± 15.3 Bq/kg as shown in column 2 of Table 4.1. This value is higher than the worldwide average activity concentration of 35 Bq/kg for ^{238}U in soil. Also, the activity concentration of ^{232}Th is highest in the HA area with an average of 179.5 ± 52.0 Bq/kg (and varies from 112.4 - 231.7 Bq/kg) while it is lowest in the PS area with an average of 63.5 ± 8.4 Bq/kg (and varies from 49.5 to 71.8 Bq/kg) as could be observed in Table 4.1 and Figure 4.1. Also, the range for the individual activity concentrations of ^{232}Th in all the 50 samples is from 49.4 to 231.7 Bq/kg as shown in Table 4.1 (column 3). The average activity concentration

of ^{232}Th from all the samples across Omaruru is 120.0 ± 42.9 Bq/kg as could be observed in Table 4.1 (column 3). These results shows that the average activity concentration of ^{232}Th in the soil of Omaruru is higher than the worldwide average activity concentration of 40 Bq/kg reported by UNSCEAR. This observation parallels the one made for ^{238}U in which the average activity concentration of ^{238}U is also higher than the worldwide average of 35 Bq/kg [46]. Correspondingly, in the case of ^{40}K its activity concentration is highest in the OA area with an average of 1325.7 ± 64.8 Bq/kg (and varies from 1247.3 to 1415.3 Bq/kg) but it is lowest in the MP area with an average of 859.4 ± 122.6 Bq/kg (and varies from 692.4 to 1008.0 Bq/kg) as could be seen in Table 4.1 column 4. The average activity concentration of ^{40}K from all the samples collected across Omaruru is 1136.7 ± 197.8 Bq/kg as could be seen in Table 4.1 (column 4). This average activity concentration of ^{40}K (from all the soil samples) is almost three times higher than the worldwide average activity concentration of 420 Bq/kg. From Figure 4.1, the activity concentration of ^{40}K (in each of the geographical areas) is much greater than those of ^{238}U and ^{232}Th while the activity concentration of ^{232}Th is higher than that of ^{238}U. It therefore follows that, of the three primordial radionuclides, ^{40}K has the highest activity concentration while ^{238}U has the least activity concentration in the soil of Omaruru. These results are consistent with those obtained in some other towns in western Namibia [2, 25].

Table 4.1 Average (± standard deviation) radionuclide concentrations in ten geographical areas of Omaruru. The range of values is given in parenthesis.

Geographical Area	**Radionuclide Concentration (Bq/kg)**		
	^{238}U	**^{232}Th**	**^{40}K**
OC	89.3 ± 21.9 (58.4 -111.1)	144.7 ± 34.8 (106.7 - 191.1)	1073.2 ± 115.5 (962.2- 1267.6)
ID	68.0 ± 7.1 (59.0 -75.2)	126.1 ± 13.3 (107.1- 144.3)	888.9 ± 49.44 (829.8-957.1)
OS	55.7 ± 9.5 (47.6 - 71.2)	97.8 ± 35.8 (67.1 - 149.7)	1260.5 ± 159.9 (1013.1 - 1425.5)
PS	48.6 ± 4.8 (43.0 - 56.3)	63.5 ± 8.4 (49.5 -71.8)	906.2 ± 75.4 (824.7 - 987.6)
MP	57.0 ± 8.6 (49.7 - 70.5)	84.8 ± 14.3 (65.9 - 103.2)	859.4 ± 122.6 (692.4 - 1008.0)
RS	56.5 ± 13.7 (39.4 - 67.2)	89.5 ± 27.5 (49.8 - 111.2)	1256.4 ± 107.2 (1089.5 - 1354.2)
OB	63.1 ± 9.4 (48.6 - 71.2)	123.9 ± 22.8 (87.3 - 143.7)	1309.4 ± 42.8 (1257.5 - 1374.5)
OA	62.1 ± 6.7 (55.2 - 70.5)	164.2 ± 16.28 (144.1 - 182.1)	1325.7 ± 64.8 (1247.3 - 1415.3)
HB	59.9 ± 4.0 (55.2 - 63.6)	125.8 ± 17.4 (110.7 - 155.0)	1244.2 ± 71.3 (1170.9 - 1318.5)
HA	78.9 ± 14.5 (62.0 - 90.8)	179.5 ± 51.9 (112.4 - 231.7)	1243.2 ± 49.8 (1155.6 - 1277.8)
Average of all samples	**63.9 ± 15.4 (39.4 - 111.1)**	**120.0 ± 42.9 (49.5 - 231.7)**	**1136.7 ± 197.8 (692.4 - 1425.5)**

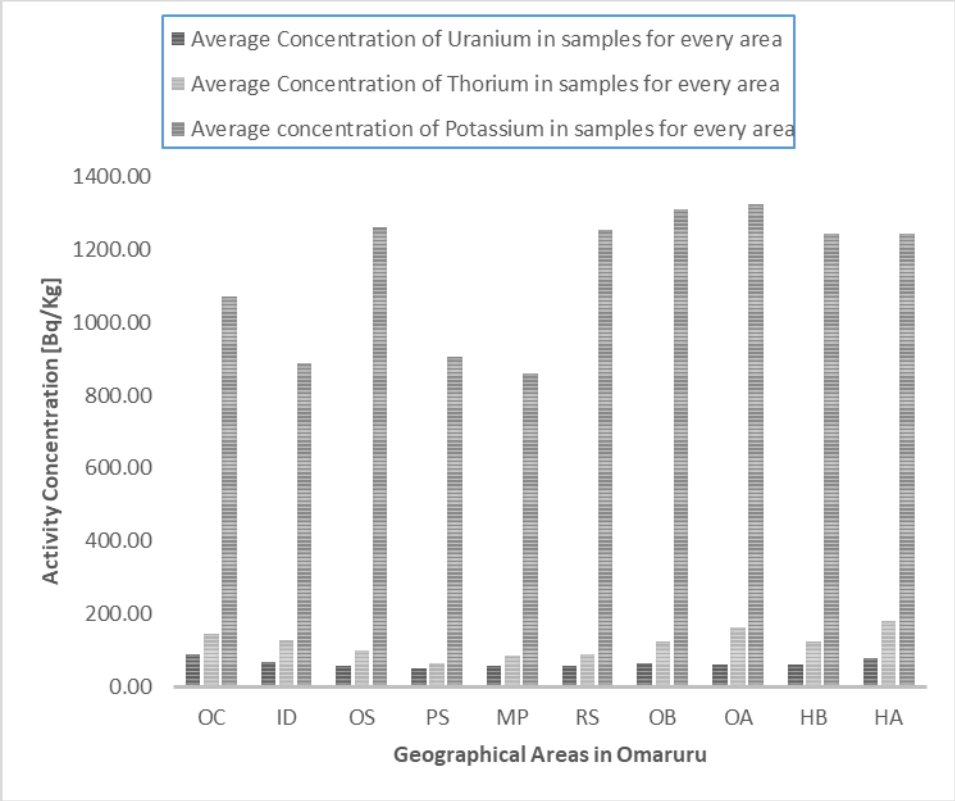

Figure 4.1 The mean activity concentrations of ^{238}U, ^{232}Th and ^{40}K in the ten geographical areas of Omaruru

Table 4.2 Statistics of the results obtained in the measurement of radioactivity in the soils of Omaruru

Descriptive Statistics	238U	232Th	40K	Absorbed dose rate	Annual effective dose rate	Radium equivalent activity	External hazard index
Standard Deviation	15.2	42.5	195.8	34.9	4.3E-02	79.3	0.2
Mean	63.9	####	1136.7	149.4	0.2	323.0	0.9
Median	61.5	117	1206.5	150.4	0.2	323.0	0.9
Standard Error	2.2	6	27.7	4.9	6.1E-03	11.2	3.0E-02
Kurtosis	1.6	0.1	-1.1	-0.3	-0.3	-0.3	-0.3
Skewness	1.2	0.5	-0.5	0.4	0.4	0.4	0.4
Maximum	111.1	232	1425.5	230.2	0.3	510.5	1.4
Minimum	39.4	49.5	692.4	90.9	0.1	189.8	0.5
Range	71.8	182	733.1	139.3	0.2	320.7	0.9

Descriptive Statistics	^{238}U	^{232}Th	^{40}K	Absorbed dose rate	Annual effective dose rate	Radium equivalent activity	External hazard index
Standard Deviation	15.2	42.5	195.8	34.9	4.3×10^{-2}	79.3	0.2
Mean	63.9	120.0	1136.7	149.4	0.2	323.0	0.9
Median	61.5	117.0	1206.5	150.4	0.2	323.0	0.9
Standard Error	2.2	6.0	27.7	4.9	6.1×10^{-3}	11.2	3.0×10^{-2}
Kurtosis	1.6	0.1	-1.1	-0.3	-0.3	-0.3	-0.3
Skewness	1.2	0.5	-0.5	0.4	0.4	0.4	0.4
Maximum	111.1	232.0	1425.5	230.2	0.3	510.5	1.4
Minimum	39.4	49.5	692.4	90.9	0.1	189.8	0.5
Range	71.8	182.0	733.1	139.3	0.2	320.7	0.9

Figure 4.2 below shows the frequency distributions of activity concentrations of (a) ^{238}U (b) ^{232}Th, and (c) ^{40}K in the 50 soil samples collected across Omaruru. As could be observed in Table 4.2 (column 2) and Figure 4.2 (a), the concentrations of ^{238}U in the soil samples have almost a leptokurtic distribution with a positive Skewness of 1.2 and a Kurtosis of 1.6. “Skewness characterizes the degree of asymmetry of a distribution around its mean. Positive skewness

indicates a distribution with an asymmetric tail extending towards more positive values. Negative skewness indicates a distribution with an asymmetric tail extending towards negative values" [46]. Similarly, "Kurtosis characterizes the relative peakedness or flatness of a distribution compared to the normal distribution. Positive kurtosis indicates a relatively peaked distribution. Negative kurtosis indicates a relatively flat distribution" [45]. From Figure 4.2 (a), the concentration of ^{238}U in most of the samples is between 47 Bq/kg and 75 Bq/kg. In fact, only eight of the 50 samples have an activity concentration greater than 75 Bq/kg while only three of the 50 samples have an activity concentration less than 47 Bq/kg. The most frequently occurring range of activity concentration of ^{238}U is 54 Bq/kg to 61 Bq/kg. As shown in Table 4.2 (column 3) and Figure 4.2 (b), the activity concentrations of ^{232}Th in the samples have almost normal distribution with a skewness of 0.5 and a kurtosis of 0.1. Also the concentration of ^{232}Th in most of the samples is between 50 Bq/kg and 165 Bq/kg, and only six samples has an activity concentration greater than 165 Bq/kg while no samples have an activity concentration smaller than 50 Bq/kg. The most frequently occurring range of activity concentration of ^{232}Th is 66 Bq/kg to 83 Bq/kg and 99 Bq/kg to 116 Bq/kg, with each range having 9 samples. Similarly, as could be seen in Table 4.2 (column 4) and Figure 4.2 (c), the activity concentrations of ^{40}K have almost a normal distribution with a negative skewness of -0.5 and a kurtosis of -1.1. The concentration of ^{40}K in most of the samples is between 766 Bq/kg and 1352 Bq/kg. Only five samples have an activity concentration greater than 1352 Bq/kg and only one sample has an activity concentration smaller than 766 Bq/kg. The most frequently occurring range of activity concentration of ^{40}K is 1279 Bq/kg to 1352 Bq/kg.

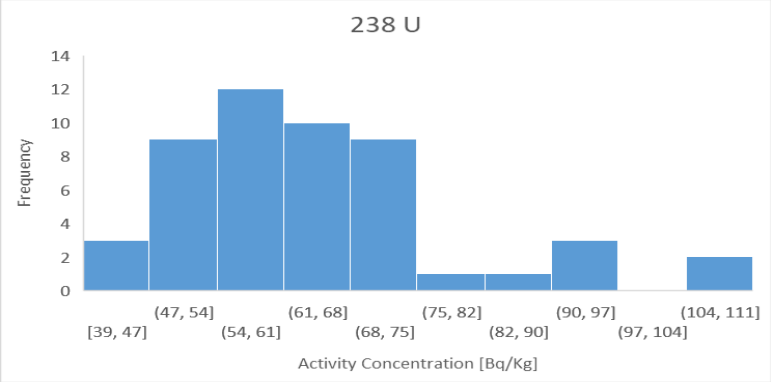

(a) ^{238}U

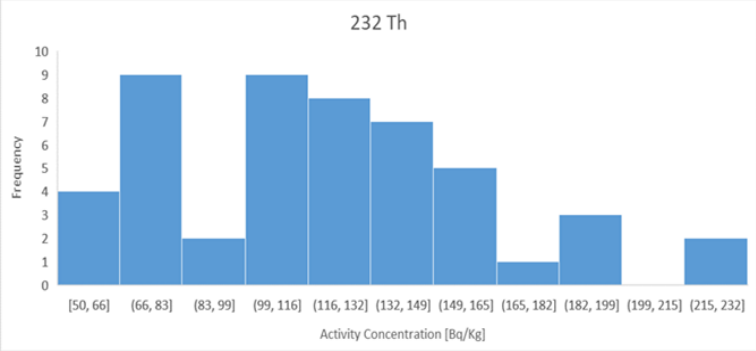

(b) ^{232}Th,

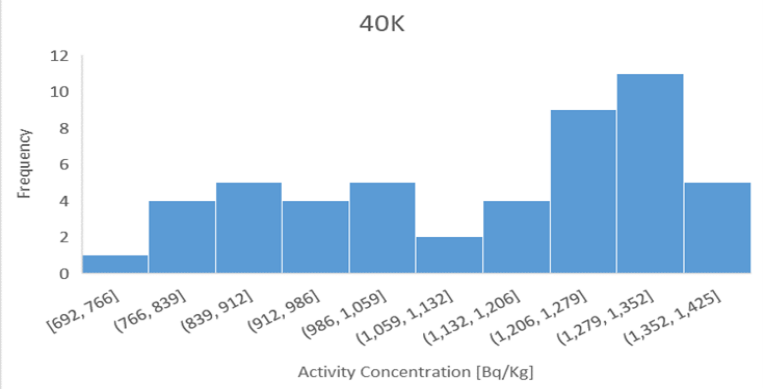

(c) ^{40}K

Figure 4.2 Frequency distributions of the concentrations of a) ^{238}U, b) ^{232}Th, and c) ^{40}K in the soil samples of Omaruru.

4.1.2 Absorbed dose rate and annual effective dose in Omaruru

The mean absorbed dose rate in air and the mean annual effective dose in each of the ten geographical areas of Omaruru are shown in Table 4.3 and Figure 4.3. As could be observed in Table 4.3 (column 2) and Figure 4.3 (a), the mean absorbed dose rate is highest in the HA area with an average value of 196.7 ± 36.6 nGy/h while it is lowest in the PS area with an average value of 98.6 ± 5.6 nGy/h. The relatively high value of the mean absorbed dose rate in the HA area is not surprising since the same area has the highest concentration of ^{232}Th in comparison with all other ten areas and relatively high concentrations of ^{238}U and ^{40}K as discussed in section 4.1.1. The average absorbed dose rate from all the ten geographical areas in Omaruru is 149.4 ± 35.3 nGy/h as shown in Table 4.3 (column 2) which is more than twice the reported worldwide average value of 60 nGy/h [46].

As could be observed in Table 4.3 (column 3) and Figure 4.3 (b) the corresponding mean annual effective dose is highest in the HA area with a value of 0.241 ± 0.045 mSv (or 241 ± 45 μSv) while it is lowest in the PS area with a value of 0.121 ± 0.007 mSv (121 ± 7 μSv). These results are not surprising since the HA and PS areas respectively have the highest and lowest absorbed dose rates. The average annual effective dose from all the ten geographical areas of Omaruru is 0.183 ± 0.043 mSv (or 183 ± 43 μSv) which is below the maximum permissible annual dose of 1.0 mSv recommended for the public by ICRP [19]. This result implies that the town of Omaruru has a normal background radiation.

Table 4.3 Mean absorbed dose rate, annual effective dose, radium equivalent activity and external hazard index in Omaruru.

Area	Mean absorbed dose rate (nGy/h)	Annual effective dose (mSv/y)	Radium equivalent activity (Bq/kg)	External hazard index
OC	173.5 ± 32.9 (140.8 - 217.7)	0.213 ± 0.040 (0.173 - 0.267)	379.0 ± 74.5 (304.7 - 477.9)	1.02 ± 0.20 (0.82 - 1.29)
ID	144.6 ± 9.6 (130.2 - 155.6)	0.177 ± 0.012 (0.160 - 0.191)	316.7 ± 22.5 (282.7 - 343.4)	0.86 ± 0.06 (0.76 - 0.93)
OS	137.4 ± 31.1 (107.3- 182.7)	0.169 ± 0.038 (0.132 -0 .224)	292.7 ± 69.9 (227.0 - 395.0)	0.79 ± 0.19 (0.61 -1 .07)
PS	98.6 ± 5.6 (90.9- 104.2)	0.121± 0.007 (0.112 - 0.128)	209.2 ± 13.4 (189.8- 223.2)	0.57 ± 0.04 (0.51 - 0.60)
MP	113.4 ± 10.9 (102.2- 127.3)	0.139 ± 0.013 (0.125- 0.156)	244.4 ± 23.5 (221.9 - 274.9)	0.66 ± 0.06 (0.60 - 0.74)
RS	132.6 ± 22.9 (102.8 - 153.6)	0.163 ± 0.028 (0.126 - 0.188)	281.2 ± 52.7 (211.3 - 328.2)	0.76 ± 0.14 (0.57 - 0.89)
OB	158.6 ± 18.1 (129.1-175.7)	0.194 ± 0.022 (0.158 - 0.216)	341.1 ± 41.6 (272.9 - 379.8)	0.92 ± 0.11 (0.74 - 1.03)
OA	183.2 ± 11.7 (169.3 - 196.3)	0.225 ± 0.014 (0.208 - 0.241)	399.0 ± 27.5 (366.0 - 429.6)	1.08 ± 0.07 (0.99 - 1.16)
HB	155.5 ± 11.4 (145.0 - 174.7)	0.191 ± 0.014 (0.178 - 0.214)	335.5 ± 26.6 (312.7 - 380.8)	0.91 ± 0.07 (0.84 - 1.03)
HA	196.7 ± 36.6 (150.9 - 230.2)	0.241 ± 0.045 (0.185 - 0.282)	431.3 ± 85.9 (323.4 - 510.5)	1.16 ± 0.23 (0.87 - 1.38)
Average of all samples	**149.4 ± 35.3 (90.9 - 230.2)**	**0.183 ± 0.043 (0.112 - 0.282)**	**323.0 ± 80.2 (189.8 - 510.5)**	**0.87 ± 0.22 (0.51 - 1.38)**

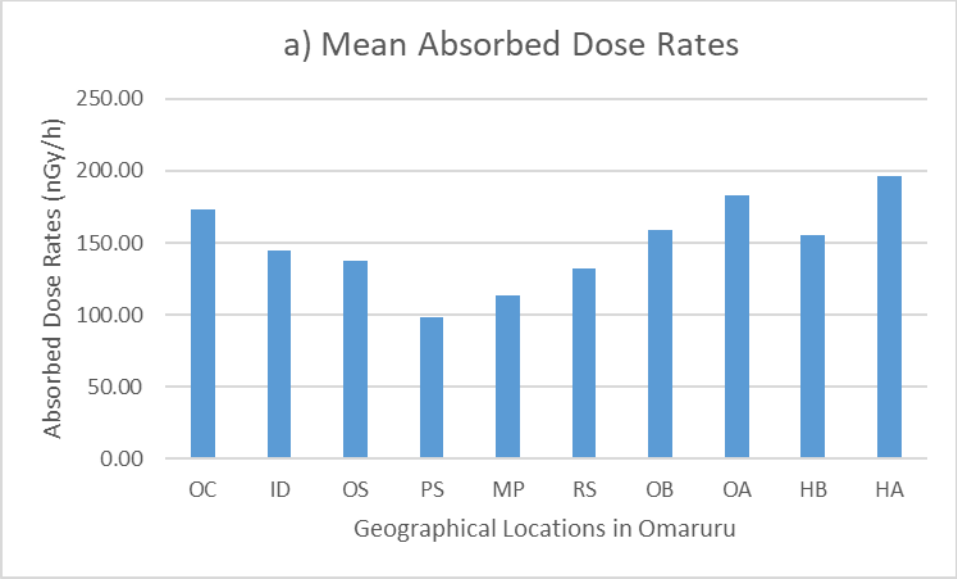

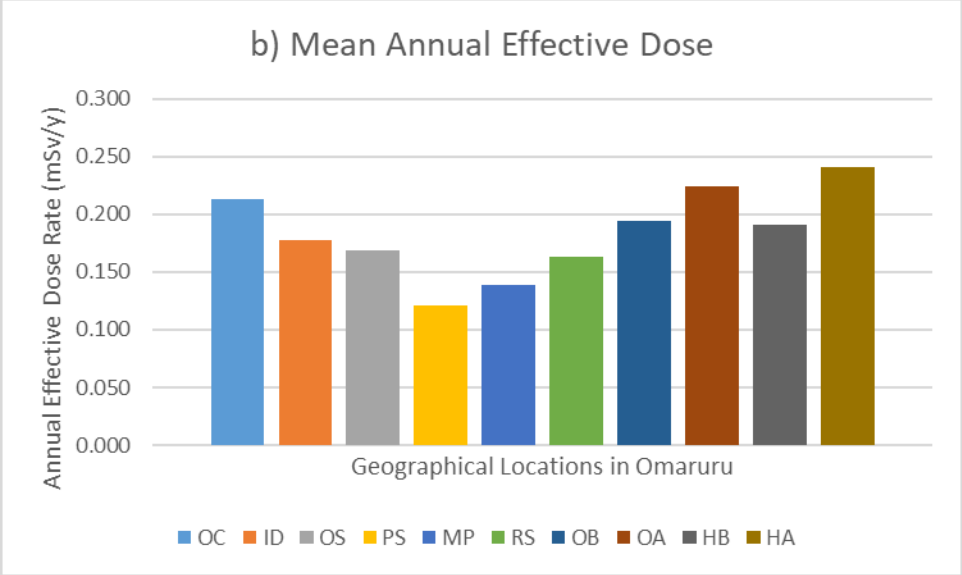

Figure 4.3: (a) The mean absorbed dose rate and (b) the mean effective dose rate in the ten geographical areas of Omaruru.

Figure 4.4 shows the frequency distributions of (a) absorbed dose rates and (b) annual effective dose in Omaruru. The absorbed dose rates have almost a normal distribution with a positive skewness of 0.4 and kurtosis of -0.3 as could be seen in Figure 4.4(a) and in Table 4.2 (column 5). The absorbed dose rate due to most of the samples is between 105 nGy/h and 216 nGy/h as could be observed in Figure 4.4 (a). Also, only three of the absorbed dose rates are greater than 216 nGy/h while seven absorbed dose rates are less than 105 nGy/h. The most frequently occurring range of absorbed dose rate is 147 to 161 nGy/h. As could be observed in Figure 4.4 (b), the annual effective dose due to most of the soil samples lies between 0.126 and 0.268 mSv. In fact, only two values of annual effective doses are greater than 0.268 mSv while four values of annual effective dose are less than 0.126 mSv.

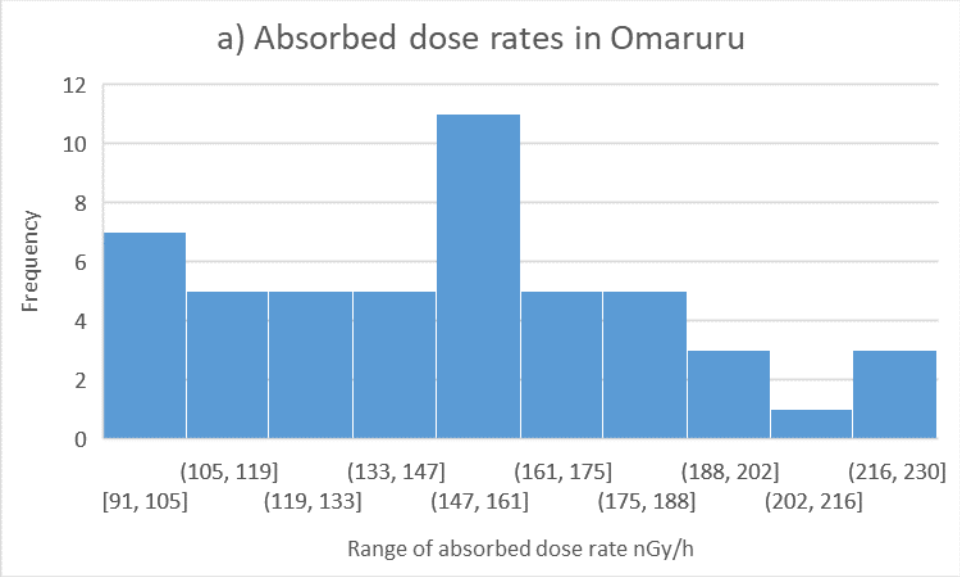

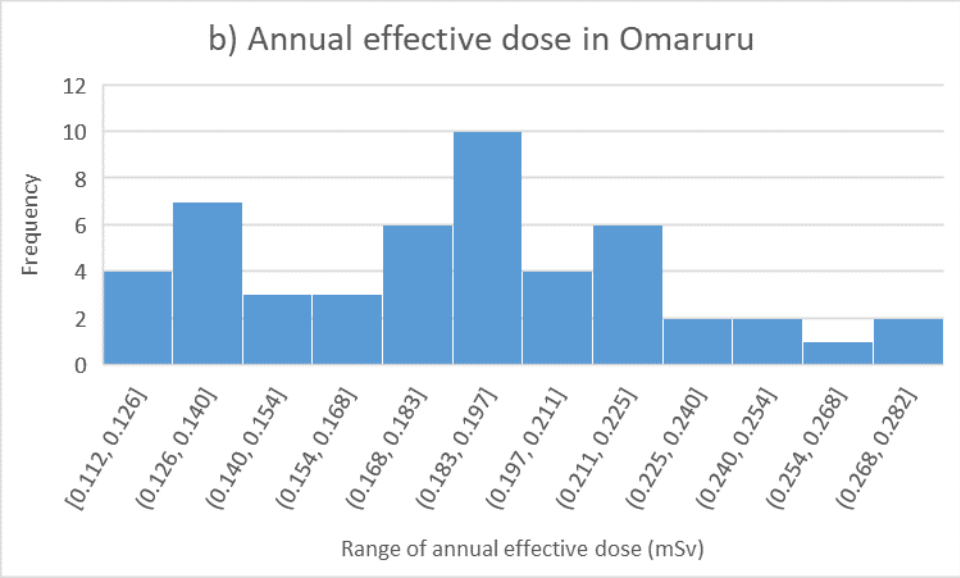

Figure 4.4: Frequency distributions of (a) absorbed dose rates and (b) annual effective dose in Omaruru.

4.1.3 Radium equivalent activity and external hazard index in Omaruru

The mean Radium equivalent activity and the external hazard index in the ten geographical areas of Omaruru are presented in Table 4.3 (columns 4 and 5) and shown in Figure 4.3. As could be seen in Table 4.3 (column 4) and Figure 4.3(a), the Radium equivalent activity is highest in the HA area with an average value of 431.3 ± 85.9 Bq/kg while it is lowest in the PS area with an average value of 209.2 ± 13.4 Bq/kg. The average Radium equivalent activity from all the ten geographical areas in Omaruru is 323.0 ± 80.2 Bq/kg. This value is below the recommended maximum of 370 Bq/kg so that radiation hazard is negligible in Omaruru [25].

Similarly, the highest external hazard index is in the HA area with an average value of 1.16 ± 0.23 while it is lowest in the PS area with an average value of 0.57 ± 0.04 as shown in Figure 4.5 (b). The average external hazard index from all the ten geographical areas is 0.87 ± 0.22. This value is less than unity thus confirming that radiation hazard is negligible in Omaruru as observed earlier in section 4.12 [28].

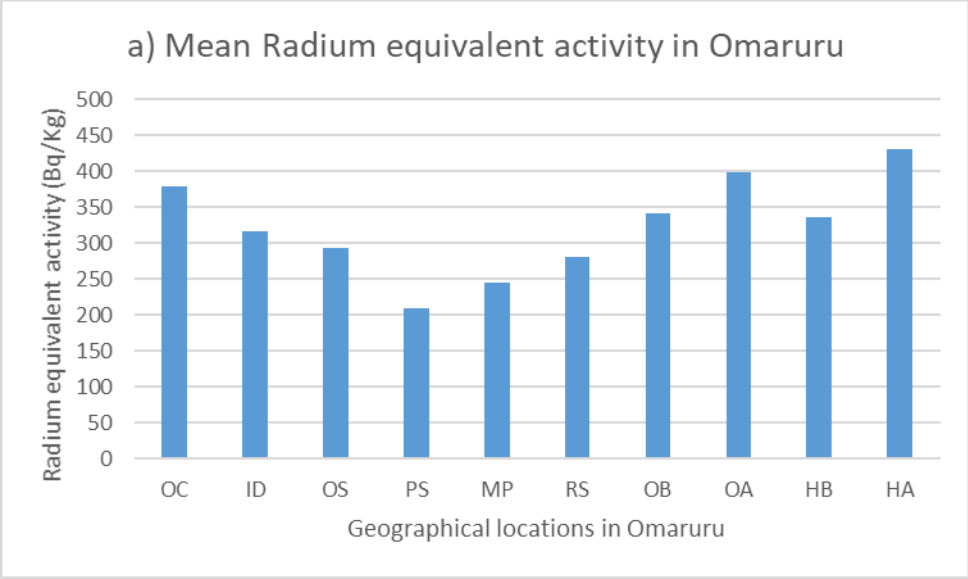

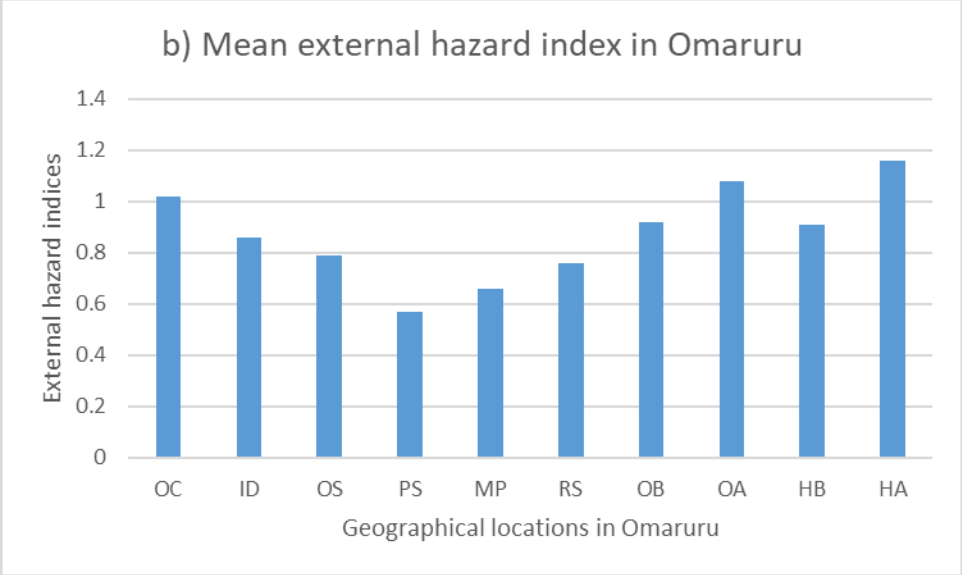

Figure 4.5: The mean Radium equivalent activity (a) and external hazard indices (b) in the ten geographical areas of Omaruru.

The frequency distributions of Radium equivalent activity and external hazard index are presented in Table 4.2 (column 7 and column 8) and shown in Figure 4.6. As could be observed in Figure 4.6 (a), most of the Radium equivalent activities calculated for the samples are between 222 Bq/kg and 478 Bq/kg. Only two samples have Radium equivalent activities greater than 478 Bq/kg and only six samples have Radium equivalent activities below 222 Bq/kg. Also, the most frequently occurring range of Radium equivalent activity is 318 to 350 Bq/kg. As could be seen in Figure 4.6 (b), most of the calculated external hazard indices are between 0.599 and 1.292. Only two of the external hazard indices are above 1.292 while five external hazard indices are below 0.599. The most frequently occurring range of external hazard index is 0.859 to 0.946. These relatively low values of H_{ex} again confirm that radiation hazard is negligible in Omaruru.

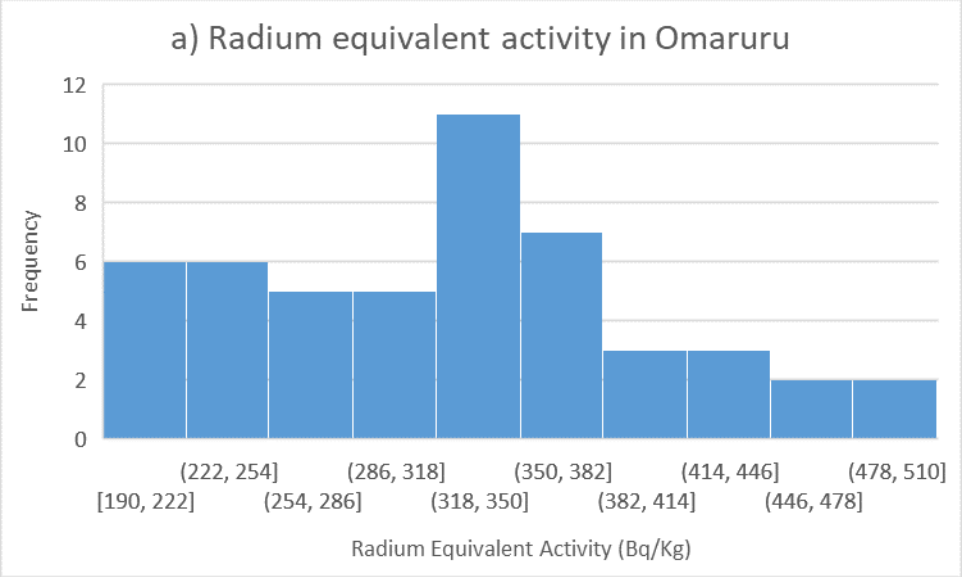

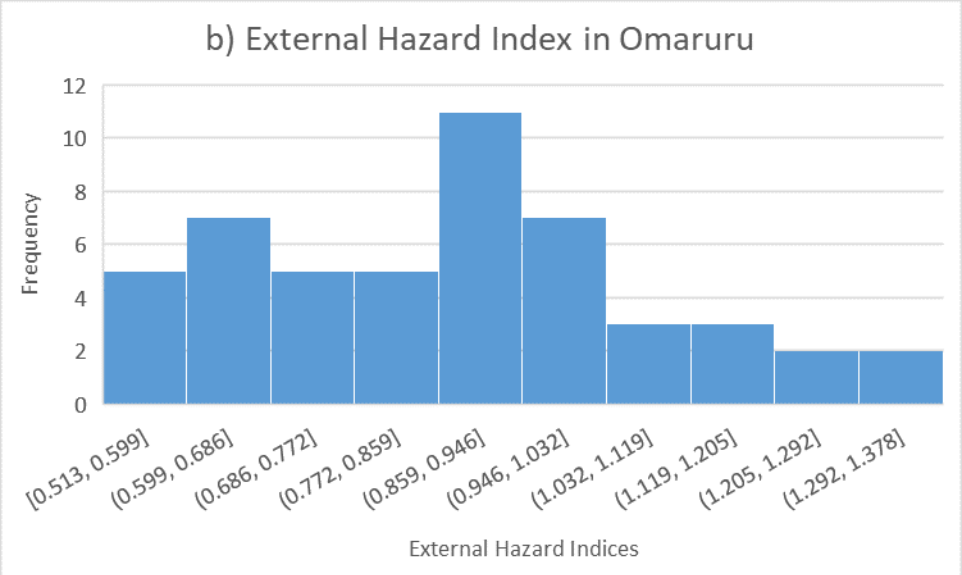

Figure 4.6: Frequency distribution of (a) Radium Equivalent activity and (b) External Hazard Index in Omaruru.

4.2 Correlation studies for the activity concentrations ^{238}U, ^{232}Th and ^{40}K

The activity concentration values for ^{238}U, ^{232}Th and ^{40}K were plotted as displayed in Figure 4.7. The relationship between the concentration of ^{238}U and ^{232}Th is shown in Figure 4.7. (a). There is a positive relationship between ^{238}U and ^{232}Th, with a correlation coefficient of 0.75, as the concentration value of ^{238}U increases, so does that of ^{232}Th. The calculated R^2 value is 0.5564.

Figure 4.7. (b) depicts the relationship between the concentration of ^{238}U and ^{40}K. ^{238}U and ^{40}K showed no significant correlation, independently from the geographical locations. The correlation coefficient is rather low, with a value of 0.08. This implies that the values of ^{238}U and ^{40}K are independent of each other and there is no visible link between the plots. The calculated R^2 value is 0.0068.

Similarly, the correlation coefficient between ^{232}Th and ^{40}K is rather low, with a value of 0.40. The relation between ^{232}Th and ^{40}K is shown in Figure 4.7. (c) and again, these values suggest weak interactions between activities of the two radionuclides, with the R^2 value being 0.1604.

Other studies have found similar trends to those found in this study [46]. Interactions between primordial radionuclides could be due to the fact that these elements are present in soil since the formation of earth. Once earth's crust solidified these radionuclides remained trapped in rocks [46].

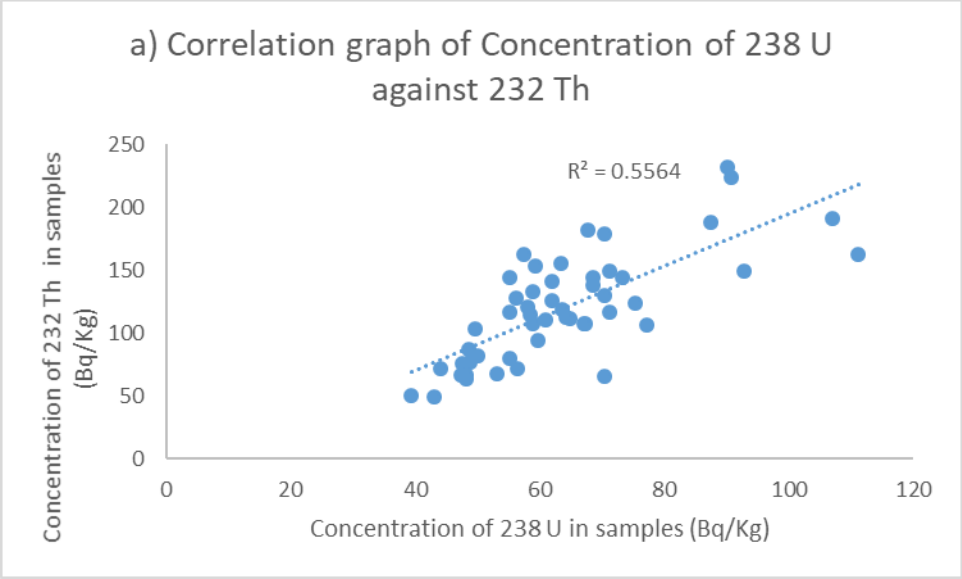
a) Correlation graph of Concentration of 238 U against 232 Th
Concentration of 232 Th in samples (Bq/Kg)
Concentration of 238 U in samples (Bq/Kg)
R² = 0.5564
0
50
100
150
200
250
0
20
40
60
80
100
120

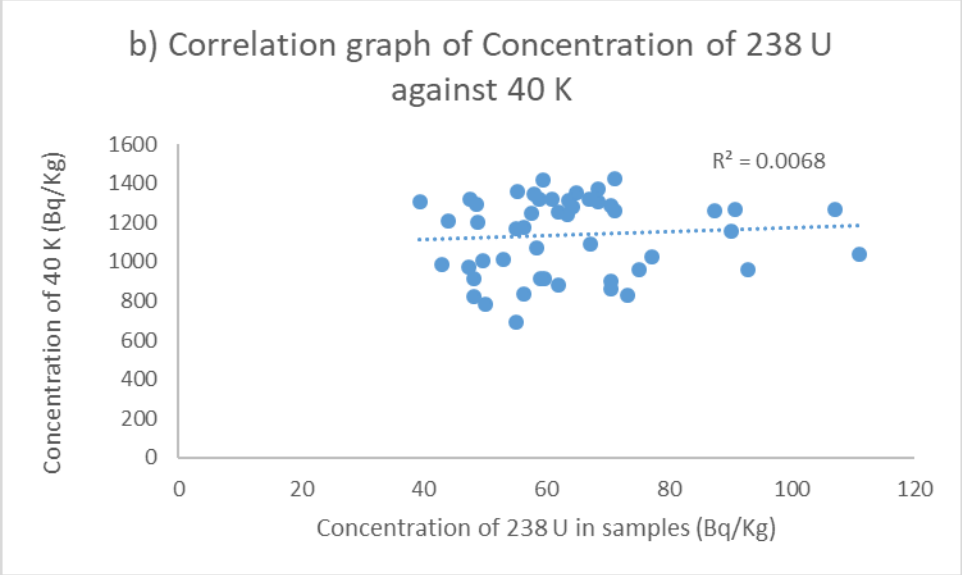
b) Correlation graph of Concentration of 238 U against 40 K
Concentration of 40 K (Bq/Kg)
Concentration of 238 U in samples (Bq/Kg)
R² = 0.0068
0
200
400
600
800
1000
1200
1400
1600
0
20
40
60
80
100
120

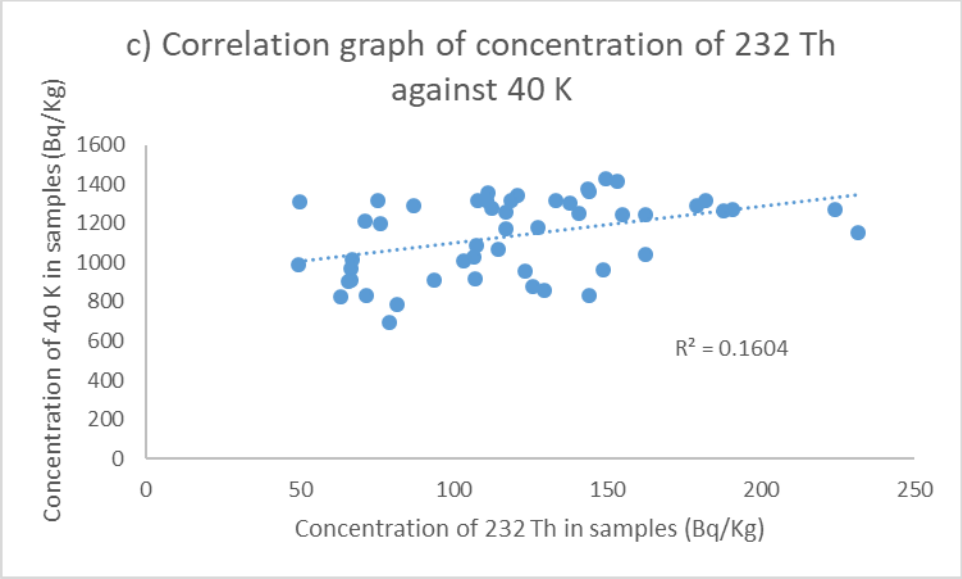

Figure 4.7. The correlation between the activity concentration of (a) ^{238}U and ^{232}Th, (b) ^{238}U and ^{40}K and (c) ^{232}Th and ^{40}K

5. Chapter 5: Conclusion

5.1 General Conclusions

In this chapter, the conclusions and suggestions for further studies are presented based on the objectives of the study. Gamma ray spectrometry has been used to study natural radioactivity in the soil of the town of Omaruru, Namibia. The town was divided into ten geographical areas and five soil samples were collected across each geographical area (giving a total of 50 samples). The activity concentrations of the primordial radionuclides ^{238}U, ^{232}Th and ^{40}K in the 50 soil samples collected were determined and used to calculate the parameters for radioactivity such as the mean absorbed dose rates, effective dose rates, radium equivalent and external hazard indices.

The mean activity concentration of ^{238}U is 63.9 ± 15.4 Bq kg^{-1} (and ranges from 39.4 to 111.1 Bq kg^{-1}). In addition, the mean activity concentration of ^{232}Th is 120.0 ± 42.9 Bq kg^{-1} (and ranges from 49.5 to 231.7 Bq kg^{-1}) while the mean activity concentration of ^{40}K is 1136.7 ± 197.8 Bq kg^{-1} (and ranges from 692.4 to 1425.5 Bq kg^{-1}).

^{238}U has the least mean activity concentration in the soils while ^{40}K has the highest mean activity concentration in the soils.

The average activity concentrations of ^{232}Th and ^{238}U are higher than world average of 40 and 35 Bq kg^{-1}, respectively. The average activity concentration of ^{40}K is higher than the worldwide average activity concentration of 400 Bq kg^{-1} by a factor of more than two.

The mean absorbed dose rate in Omaruru is 149.4 ±35.3 $nGyh^{-1}$ and the corresponding mean effective dose rate is 0.183 ± 0.043 mSv/year.

The absorbed dose rates in the town is higher than the worldwide average value of 60 $nGyhr^{-1}$. The corresponding mean effective dose rate in the town of Omaruru is far below the maximum permissible value of 1.0 mSv/year. This result implies that the town of Omaruru has normal background radiation. The mean Radium equivalent activity is 323.0 ± 80.2 $Bqkg^{-1}$. The value is much lower than the recommended value of 370 Bq/kg thus confirming the town of Omaruru has a normal background radiation. The average external hazard index determined for Omaruru is 0.87 ± 0.22. This value is again less than the recommended safe level of unity. This result further confirms that radiological hazard is low.

The results obtained in this study will be useful in establishing a baseline data on the activity concentrations of ^{238}U, ^{232}Th and ^{40}K in selected towns in Namibia, which will be useful as a reference in assessing changes in environmental radioactivity in future.

5.2. Recommendations and Suggestions for Further Research

A similar but more detailed study is highly recommended for the entire Namibia. This should be extended to cover activity levels in plants and water. Various plants used for food or otherwise should be considered for this study. Sources of water used for drinking and cleaning purposes.

Further study should also be carried out to determine levels of the indoor component of annual effective radiation exposure dose. Since exposures to natural radiation sources are more significant for the world's population than most exposures to man-made sources, the natural background baseline warrants evaluation in some detail. Efforts should continue to broaden the database used for determining both representative values and extremes in exposures and to improve dosimetric procedures. Because of the wide variations in natural background exposures even within relatively small regions, more efforts will be required to determine the detailed distributions of populations

within dose intervals for the various components of exposure. These evaluations seem to reveal patterns that would be expected to be generally valid for other countries and for the world population as a whole. The analysis of distributions will provide an improved basis for deriving worldwide average exposures and their normal and extreme variations.

References

1.Shanthi, G., Kumaran, J. T. T., Raj, G. A. G. and Maniyan, C. G. (2010). Measurement of activity concentration of natural radionuclides for the assessment of radiological indices. *Radiation Protection Dosimetry.*

2. Shimboyo, S. A., Oyedele, J. A. and Sitoka, S. S. (2016). Soil radioactivity levels and associated hazards in selected towns in uranium-rich western Namibia. *International Science and Technology Journal of Namibia.*

3. Kovács, T., Szeiler, G., Fábián, F., Kardos, R. and Gregorič, A. (2013). Systematic survey of natural radioactivity in soil in Slovenia. *Journal of Environmental Radioactivity*, pp. 70-78.

4. Oyedele, J. A., Sitoka, S. and Davids, I. (2008). Radionuclide concentrations in soils of Northern Namibia, Southern Africa. *Journal of Radiation Protection Dosimetry*, pp. 482-486.

5. Withanage, A.P., Mahawatte, P. (2013). Radioactivity of beach sand in the south western coast of Sri Lanka. *Radiation Protection Diosimetry*.Vol.153

6. Papaefthymiou, H.V., Manousakas, M., Fouskas, A,.and Siavalas, G. (2013). Spatial and vertical distribution and risk assessment of natural radionuclides in soils surrounding the lignite-fired power plants in megalopolis basin, Greece. *Radiation Protection Dosimetry*. Vol.156

7. Nayyeri, V., Hashemi, S.M., Borna, M., Jalilian, H. and Soleimani, M. (2013). Assessment of radiation levels in the vicinity of 60 GSM mobile phone base stations in Iran. *Radiation Protection Dosimetry*. Vol.155

8. Miller. Namibian Geology Miller Series.

9. Carvalho, P.F., Matine, O.F., Taimo, S., Oliveira, J.M., Silva, L., and Malta, M. (2013). Radionuclides and Radiation Doses in Heavy Mineral Sands and other Mining Operations in Mozambique. *Radiation Protection Dosimetry*.

10. Maphoto, K.P. (2004). Determination of Natural Radioactivity Concentrations in Soil: a comparative study of Windows and Full Spectrum Analysis.

11. Gedeon, G., P. E. Nuclear Physics and Reactor Theory, Module 1: Atomic and Nuclear Physics. Department of Energy.

12. Bailey, D.L., Humm, J.L., Todd-Pokropek, A., Van Aswegen, A. (2014) Nuclear Medicine Physics, A Handbook for Teachers and Students. International Atomic Energy Agency.

13. Von Oertzen, G. and Von Oertzen D. (2018) Radiation Safety Officer's Handbook.

14. Midzi, W. (2018). An Evaluation of the Natural Radioactivity in the Soils of Okahandja and Karibib, Namibia.

15. Environmental Radioactivity: from natural, industrial and military sources. Merril E., Thomas G. fouth edition, San Diego : *Academic press publishers* , 1997.

16. UNSCEAR (1993). Sources and effects of ionizing radiation. 1993 Report to the General Assembly, with scientific annexes. United Nations Scientific Committee on the Effects of Atomic Radiation. United Nations, New York

17. De Jong, P. (2010). Exposure to natural radioactivity in the Netherlands; the impact of building materials, Goroningen Netherlands.

18. United Nations Scientific Committee on The Effects of Atomic. Sources and effects of ionizing radiation. New York : UNSCEAR. (2000). Sources and effects of ionizing radiation. United

Nations Scientific Committee on The Effects of Atomic Radiation, Report to the General Assembly, Natural Radioactivity Publications: Annexure B: Sources. New York: United Nations., 2000.

19. ICRP publication 103 Ann, 2007.

20. WHO (2006) Health effects of the Chernobyl accident and special health care programmes. Report of the UN Chernobyl Forum Expert Group "Health". Eds. Bennett, B., Repacholi, M. and Carr, Z. World Health Organization, Geneva.

21. Issa, S.M. (2013). Radiometric Assessment of natural radioactivity levels of agricultural soil samples collected in Dakahlia, Egypt. *Radiation Protection Dosimetry*, Vol. 156.

22. El Samad, O., Baydoun, R., Nsouli, B., Darwish, T. (2013). Determination of natural and artificial radioactivity in soil at North Lebanon province Beirut, Lebanon. *Journal of Environmental Radioactivity*. Vol. 125.

23. Duggal, V., Ranu, A., Mehra, R. and Ramola, R.C.(2013). Assessment of Natural Radioactivity Levels and Associated Dose Rates in Soil Samples from Northern Rajasthan India Rajasthan, India. *Radiation Protection Dosimetry*.

24. Cam, N.F., Ozken, I., Yaprak, G. (2012). A survey of natural radiation levels in soils and rocks from Aliaga-Foca Region in Izmir, Turkey. *Radiation Protection Dosimetry*, Vol. 155.

25. Shimboyo, S.A. (2013). Natural radioactivity in soils of the Walvis Bay-Henyies Bay coastal area, Namibia. Masters dissertation, University of Namibia.

26.Tubosun, I. A., Tchokossa, P., Balogun, F. A., Fasasi, M. K., Ocan, O. and Adesanmi, C. A. (2013). Natural radioactivity in some rocks employed as dimension and decorative stones in the Nigerian building industry. *Journal of Radiation Protection Dosimetry*.

27. Najam, L.A., Karim, S.M., and Hameed, T.K. (2016). Evaluation of natural radioactivity of soil samples from different regions of wassit governance. Baghdad, Iraq.

28. Mohammed, K., Mohanad, T., Jazzar M .(2012). Natural Radioactivity Levels and Estimation of Radiation Exposure in Environmental Soil Samples from Tulkarem Province-Palestine. *Open Journal of Soil Science*.

29. Ateba, J.F.B., Ateba, P.O., Ben-Bolie, G.H., Ele-Abiama, P., Abega, C.R. and Mvondo S.(2010).Natural background dose measurements in south Cameroon. *Radiation Protection Dosimetry*, Vol. 140.

30. Abdullahi, M. A., Mohammed, S.S. and Iheakanwa, I. A. (2013). Kaduna Measurement of Natural Radioactivity in Soil Along the Bank of River Kaduna – Nigeria. *American Journal of Engineering Research (AJER).*

31. Mehra, R., Badhan, K., Sonkawade, R.G., Kansal S and Singh, S. (2010). Analysis of terrestrial natural radionuclides in soil samples and assessment of average effective dose Punjab, India. *Indian Journal of Pure and Applied Science*, Vol. 48.

32. Alazemi N, Bajoga A D, Bradley D A, Regan P H and Shams H. (2016) Soil radioactivity levels, radiological maps and risk assessment for the state of Kuwait. *Chemosphere* 154 55–62

33. Nkoulou II, J.E.N., Talla, F.S., Bineng, G.S., Manga, A., Siaka, Y.F.T and Saïdou.(2018) Natural Radioactivity Measurements in Soil, External Doseand Radiological Hazard Assessment

in the Uranium and Thorium Bearing Region of Lolodorf, Cameroon.Yaoundé. *RADIOISOTOPES,* Vol. 67.

34. Mujahid, S.A., and Hussain, S. (2010) Natural radioactivity in soil in the Baluchistan Province of Pakistan. *Radiation Protection Dosimetry*, 2010, Vol.140. pp 333-339.

35. Kebwaro, J., Rathorel, I., Hashim, N., & Mustapha, A. Mirma. (2011). Radiometric assesment of natural radioactivity levels around Mirma Hill, Kenya. *International Journal of the Physical Sciences*, 2011, Vol. 6(13). 3105-3110.

36. Fatima, I., Zaidi H.J., Arif, M., Daud, M., Ahmad, S.A and Tahir, S.N.A. (2007). Measurement of natural radioactivity and dose rate assessment of terrestrial gamma radiation in the soil of southern Punjab, Pakistan. *Radiation Protection Dosimetry*. Vol. 128.

37. Bilgici, G., Caglar, A. (2017). Evaluation of natural radioactivity levels and radiological hazards in soil samples of Sarikamis Province,Kars, Turkey. *Radiation Science and Technology.*

38. Maps Namibia. Retrieved September 14 2020, from https://images.app.goo.gl/VFd4V6EyWpYJmS827.

39. Atlas of Namibia Project (2002). Directorate of Environmental Affairs. Ministry of Environment and Tourism.

40. Dominant Soils in Namibia. Atlas of Namibia Project 2002. Directorate of Environmental Affairs. Ministry of Environment and Tourism.

41. Chauhan, Pooja and R.P., (2012). Elemental analysis of fertilizers using x-ray fluorescence and their impact on alpha radioactivity of plants. Journal of Radioanalytical and Nuclear Chemistry. 295. 10.1007/s10967-012-2244-6

42. Hendriks P.H.G.M., Limburg J., de Meijer R.J., (2001). Full-spectrum analysis of natural gamma-ray spectra, *Journal of Environmental Radioactivity* 53, 365.

43. IAEA, Tec-Doc-1363, 2000

44. Gordon R. G. (2008). Practical Gamma-ray Spectrometry, 2nd Edition, *John Wiley & Sons*, Britain.

45. Redmond, WA. Microsoft [Computer software].Excel. . s.l. : Microsoft corporation, 1996.

46. United Nations Scientific Committee on The Effects of Atomic. Sources and effects of ionizing radiation. New York: UNSCEAR. (2000*). Sources and effects of ionizing radiation. United Nations Scientific Committee on The Effects of Atomic Radiation, Report to the General Assembly, with Scientific Annexes*, Vol.I: Sources. New York: United Nations., 2000.

47. Nicola, P. (2011). Activity concentration and transfer factors of natural and artificial radionuclides in the Swedish counties of Uppsala and Jämtland. University of Copenhagen, Denmark.

Appendix A

Isotope Concentrations in Omaruru							
s/n	Area	Concentration of Uranium in sample (Bq/kg)	Error in concentration of Uranium value	Concentration of Thorium in sample (Bq/kg)	Error in concentration of Thorium value	Concentration of Potassium in sample (Bq/kg)	Error in concentration of Potassium value
1	OC	107.1	3.8	191.1	8.7	1267.6	46.0
2	OC	111.1	3.7	162.5	7.6	1038.5	38.8
3	OC	92.8	3.6	148.8	7.1	962.2	36.6
4	OC	58.4	2.7	114.7	6.1	1069.1	39.5
5	OC	77.3	3.2	106.7	5.7	1028.4	38.6
6	ID	75.2	3.3	123.5	6.5	957.1	36.3
7	ID	73.2	3.0	144.3	7.1	829.8	32.7
8	ID	62.0	3.2	125.8	5.9	880.7	34.3
9	ID	59.0	2.8	107.1	6.1	916.4	35.1
10	ID	70.5	3.1	129.5	6.6	860.4	33.4
11	OS	71.2	3.4	149.7	6.7	1425.5	50.6
12	OS	58.0	3.0	120.7	6.7	1344.0	48.1
13	OS	53.1	2.6	67.1	4.9	1013.1	38.0
14	OS	47.6	2.8	75.4	5.1	1318.5	47.0
15	OS	48.8	2.6	76.3	5.3	1201.5	43.5
16	PS	47.4	2.5	66.7	4.3	972.4	36.6
17	PS	48.2	2.5	63.2	4.2	824.7	32.4
18	PS	43.0	2.3	49.5	4.4	987.6	36.9
19	PS	56.3	2.6	71.8	4.9	834.9	32.5
20	PS	48.2	2.5	66.5	4.8	911.3	34.7
21	MP	70.5	3.0	65.9	4.5	901.1	34.6
22	MP	59.8	3.1	93.6	5.2	911.3	35.0
23	MP	49.7	2.8	103.2	5.6	1008.0	37.7
24	MP	50.1	2.6	81.9	5.0	784.0	31.3
25	MP	55.2	2.6	79.3	4.8	692.4	28.5
26	RS	67.2	3.0	107.4	6.1	1089.5	40.6
27	RS	39.4	2.5	49.8	4.2	1308.4	46.6
28	RS	64.9	2.8	111.2	6.3	1354.2	48.2
29	RS	67.0	3.0	107.7	6.1	1318.5	47.1
30	RS	44.0	2.7	71.3	5.0	1211.6	43.6
31	OB	68.4	3.5	138.1	6.8	1303.3	46.8
32	OB	58.8	2.9	133.3	6.9	1318.5	47.1
33	OB	48.6	2.5	87.3	5.5	1293.1	46.3
34	OB	71.2	3.2	117.1	6.7	1257.5	45.7
35	OB	68.4	2.9	143.7	6.5	1374.5	48.8
36	OA	70.5	3.3	179.1	8.3	1288.0	45.8
37	OA	55.2	2.9	144.1	7.0	1359.3	48.2
38	OA	67.8	3.0	182.1	8.2	1318.5	47.0
39	OA	57.5	2.7	162.5	7.9	1247.3	44.9
40	OA	59.4	3.3	153.5	7.4	1415.3	49.9
41	HB	60.9	2.7	110.7	6.2	1318.5	47.3
42	HB	55.2	3.0	117.1	6.5	1170.9	42.7
43	HB	63.5	2.9	155.0	7.3	1242.2	45.0
44	HB	63.6	3.0	118.6	6.3	1313.5	46.8
45	HB	56.2	2.9	127.4	6.1	1176.0	42.9
46	HA	62.0	2.8	141.0	7.4	1252.4	45.2
47	HA	64.3	3.1	112.4	6.0	1277.8	45.9
48	HA	90.1	3.3	231.7	9.2	1155.6	42.4
49	HA	90.8	3.9	224.2	8.9	1267.6	45.9
50	HA	87.4	2.4	188.1	8.4	1262.5	45.7

Appendix B

E-mail muniomar@iway.na
Namibia

OFFICE OF THE CHIEF EXECUTIVE OFFICER

Enquiries: Mr. Alphons Tjitombo

Our Ref: CEO-04/17-2018/UNAM
Your ref: None

24 April 2018

UNIVERSITY OF NAMIBIA
FACULTY OF SCIENCE: DEPARTMENT OF PHYSICS
Private Bag 13301
WINDHOEK
Namibia

Dear Oyedele,

REQUEST TO TAKE SOIL SAMPLE IN OMARURU

The above matter herein refers.

This letters serves to inform your esteem office that your application to collect soil samples in Omaruru during 25-26 April 2018 as per your request has been granted. This information will be shared with the Board Chairperson, Her Worship the Mayor of Omaruru Hendrina Magano Gebhardt.

Thanking you in advance.

Yours truly,

Alphons Tjitombo
Chief Executive Officer

ALL OFFICIAL CORRESPONDANCES MUST BE ADDRESSED TO THE OFFICE OF THE CHIEF EXECUTIVE OFFICER 2018

Appendix C

FACULTY OF SCIENCE: DEPARTMENT OF PHYSICS
University of Namibia, Private Bag 13301, Windhoek, Namibia
340 Mandume Ndemufayo Avenue, Pioneers Park
☎ +264 61 206 3673; Fax: +264 61 206 3791; URL.: http://www.unam.edu.na

UNAM
UNIVERSITY OF NAMIBIA

April 23, 2018.

Mr Alphons Tjitombo
The Chief Executive Officer
Omaruru Town Council
P O Box 14
Omaruru

Dear Sir,

REQUEST FOR PERMISSION TO TAKE SOIL SAMPLES IN OMARURU

I wish to apply for your permission to take some small soil samples from different parts of Omaruru for research studies at the University of Namibia (UNAM).

A research group in the Physics Department of UNAM is interested in studying soils in different parts of the Country and will therefore like to take a small amount of soil (about one kilogram) from different sites in Omaruru during the period 25-26 April 2018. The activity will not affect the landscape and does not have any financial implication for the town. In fact, the results of the study will be made available to the town and should benefit Omaruru.

Thank you.

Professor James Oyedele,
Department of Physics.

Cell: 0812554025
Phone: (061) 206-3373
Fax: (061) 206-3791

OMARURU MUNICIPALITY
Tel: +264 64 570022
Fax +264 64 570105
2018 -04- 25
Sign:.....
OFFICE OF THE CEO

APPROVED BY: ALPHONS TJITOMBO

Appendix D

Python Program to calculate activity concentrations

```
# Program to calculate concentrations, Dose rate and Anual effective dose from the isotopes U-238, Th-232 and K-40

import math
import numpy as np
import pandas as pd


df = pd.read_csv("DataM.csv")

U = df.Uranium

Th = df.Thorium

K = df.Potassium

Uer = df.U_error

Ther = df.Th_error

Ker = df.K_error


As_U = 72600.0 # Net peak area in RGU standard

Cs_U = 4940.0 # Concentration of U in Bq/kg in RGU standard

k_U = As_U/Cs_U # k standard for U-238

ke_U = 0.1078371077          # error in k standard for U-238


As_Th = 22600.0 # Net peak area in RGTh standard

Cs_Th = 3250.0 # Concentration of Th in Bq/kg in RGTh standard

k_Th = As_Th/Cs_Th # k standard for Th-232

ke_Th = 0.1984386424          # error in k standard for Th-232
```

```
As_K = 27000.0 # Net peak area in RGK standard

Cs_K = 14000.0 # Concentration of K in Bq/kg in RGK standard

k_K = As_K/Cs_K # k standard for K-40

ke_K = 0.05634388545        # error in k standard for K-40

# Radionuclide concentrations and their errors

U_concn = U/k_U

U_concn_er = U_concn*(((Uer/U)**2 + (ke_U/k_U)**2)**0.5)

Th_concn = Th/k_Th

Th_concn_er = Th_concn*(((Ther/Th)**2 + (ke_Th/k_Th)**2)**0.5)

K_concn = K/k_K

K_concn_er = K_concn*(((Ker/K)**2 + (ke_K/k_K)**2)**0.5)

# Radiological hazards

Dt = 0.042* K_concn + 0.429*U_concn + 0.666*Th_concn

Dt_er = ((0.042*K_concn_er)**2 + (0.429*U_concn_er)**2 + (0.666*Th_concn_er)**2)**0.5

A_eff_Dose = Dt*0.00876*0.7*0.2

A_eff_Dose_er = Dt_er*0.00876*0.7*0.2
```

```
R_eqq_Dose = U_concn + 1.43*Th_concn + 0.077*K_concn

R_eqq_Dose_er =  U_concn_er + 1.43*Th_concn_er + 0.077*K_concn_er


Ex_H_index = (Th_concn/259) + (U_concn/370) + (K_concn/4810)

Ex_H_index_er = (Th_concn_er/259) + (U_concn_er/370) + (K_concn/4810)


In_H_index = (Th_concn/259) + (U_concn/185) + (K_concn/4810)

In_H_index_er = (Th_concn_er/259) + (U_concn_er/185) + (K_concn_er/4810)


z = open ('Mresults.csv','w')

z.write ('U_cn , U_cn_er , Th_cn , Th_cn-er , K_cn  , K_cn_er , Dse_rt , Dse_rt_er , A_ef_dse ,
A_ef_dse_er , R_eqq_dse , R_eqq_dse_er , Ex_Hin , Ex_Hin_er , In_Hin , In_Hin_er , \n')

i= 0

for i in range (0,50):

   z.write ('%2.2f , %2.2f , %2.2f , %2.2f , %2.3f , %2.2f , %2.2f , %2.2f , %2.3f , %2.3f , %2.2f ,
%2.2f , %2.2f , %2.2f , %2.2f , %2.2f, \n'%(U_concn[i], U_concn_er[i],Th_concn[i],
Th_concn_er[i], K_concn[i], K_concn_er[i], Dt[i], Dt_er[i], A_eff_Dose[i],
A_eff_Dose_er[i],R_eqq_Dose[i],R_eqq_Dose_er[i],Ex_H_index[i],
Ex_H_index_er[i],In_H_index[i],In_H_index_er[i]))

i += 1

z.close()
```